JOC*Article*

Dialkoxyphosphinyl-Substituted Enols of Carboxamides

Jinhua Song,[†] Hiroshi Yamataka,[‡] and Zvi Rappoport*,[†]

Department of Organic Chemistry and the Lise Meitner Minerva Center for Computational Quantum Chemistry, The Hebrew University, Jerusalem 91904, Israel, and Department of Chemistry, Rikkyo University, Nishi-Ikebukuro 3-34-1, Toshima-ku, Tokyo, 171-8501, Japan

zr@vms.huji.ac.il

Received May 23, 2007

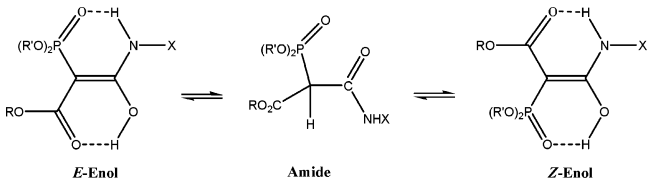

R = Me, CF_3CH_2, $(CF_3)_2CH$; R' = Me, CF_3CH_2

Reactions of isocyanates XNCO (e.g., X = *p*-An, Ph, *i*-Pr) with $(MeO)_2P(=O)CH_2CO_2R$ [R = Me, CF_3CH_2, $(CF_3)_2CH$] gave 15 formal "amides" $(MeO)_2P(=O)CH(CO_2R)CONHX$ (**6**/**7**), and with $(CF_3CH_2O)_2P(=O)CH_2CO_2R$ [R = Me, CF_3CH_2] they gave eight analogous amide/enols **17**/**18**. X-ray crystallography of two **6**/**7**, R = $(CF_3)_2CH$ systems revealed *Z*-enols of amides structures $(MeO)_2P(=O)C(CO_2CH(CF_3)_2)=C(OH)NHX$ **7** where the OH is cis and hydrogen bonded to the $O=P(OMe)_2$ group. The solid phosphonates with R = Me, CF_3CH_2 have the amide **6** structure. The structures in solution were investigated by ^1H, ^{13}C, ^{19}F, and ^{31}P NMR spectra. They depend strongly on the substituent R and the solvent and slightly on the *N*-substituent X. All systems displayed signals for the amide and the *E*- and *Z*-isomers. The low-field two δ(OH) and two δ(NH) values served as a probe for the stereochemistry of the enols. The lower field δ(OH) is not always that for the more abundant enol. The % enol, presented as K_{enol}, was determined by ^1H, ^{19}F, and ^{31}P NMR spectra, increases according to the order for R, Me < CF_3CH_2 < $(CF_3)_2CH$, and decreases according to the order of solvents, CCl_4 > $CDCl_3$ ~ THF-d_8 > CD_3CN > DMSO-d_6. In DMSO-d_6, the product is mostly only the amide, but a few enols with fluorinated ester groups were observed. The *Z*-isomers are more stable for all the enols **7** with *E*/*Z* ratios of 0.31−0.75, 0.15−0.33, and 0.047−0.16 when R = Me, CF_3CH_2, and $(CF_3)_2CH$, respectively, and for compounds **18**, R = Me, whereas the *E*-isomers are more stable than the *Z*-isomers. Comparison with systems where the $O=P(OMe)_2$ is replaced by a CO_2R shows mostly higher K_{enol} values for the $O=P(OMe)_2$-substituted systems. A linear correlation exists between δ(OH)[*Z*-enols] activated by two ester groups and δ(OH)-[*E*-enols] activated by phosphonate and ester groups. Compounds $(MeO)_2P(=O)CH(CN)CONHX$ show $\leq$7.3% enol in $CDCl_3$ solution. For $[(MeO)_2P(=O)]_2CHCONHX$, activated by two $O=P(OMe)_2$ groups, only the amides were observed in solution and in the solid. DFT calculations reproduce the general effect of R on K_{enol}, but the correlation between observed and calculated K_{enol} values is not linear. The roles of electron withdrawal by the activating phosphonate and ester groups, and the importance of N−H and O−H hydrogen bonding to them in stabilizing the enols are discussed.

Introduction

Simple enols of carboxamides are very unstable compared with their isomeric amides. For example, the calculated equilibrium constant K_{enol} = [enol]/[amide] between the parent acetamide CH_3CONH_2 and its enol $CH_2=C(OH)NH_2$ is $10^{-21.6}$,[1] and hence, the enol and related enols are unobservable by spectroscopic techniques such as NMR at room temperature. Increase of the stability by substitution with two β-bulky aromatic substituents increases K_{enol} appreciably, but even then the enol of amide is observable by NMR or UV spectroscopy

[†] The Hebrew University.
[‡] Rikkyo University.

(1) Sklenak, S.; Apeloig, Y.; Rappoport, Z. *J. Am. Chem. Soc.* **1998**, *120*, 10359.

10.1021/jo0710679 CCC: $37.00
Published on Web 08/31/2007

only rarely, and if at all, as a short-life or medium-life intermediate of some kinetic but not thermodynamic stability.[2,3] In recent years, we used a different method and increased the stability of the enols by substituting C_β with two electron-withdrawing groups (EWGs) by resonance Y and Y′. The contributing dipolar push−pull structure **1b** to the enol hybrid **1a**/**1b** is much more stabilizing than the contributing structure **2b** to the amide hybrid **2a**/**2b**, and the right-hand side of eq 1 becomes frequently more stabilized than the left-hand side, giving in favorable cases observable enols of amides with easily measured K_{enol} values and isolable enols in several systems.

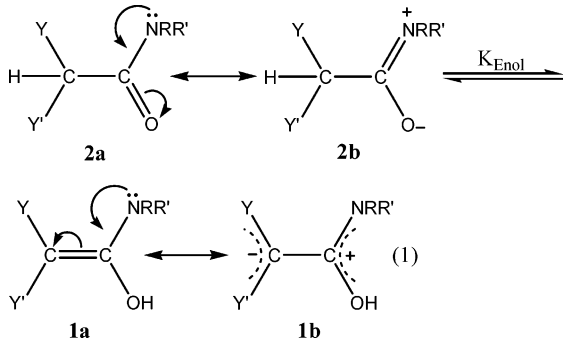

Enols of amides were isolated and their solid-state structures determined when YY′ = Meldrum's acid[4,5] or indandione[6] moieties or when Y,Y′ = CO_2R,CO_2R'';[4,5,7c] CN,CN;[8] CN,-CO_2R;[7,8] CN,$CONR^1R$,[9] CN,$CSNR^1R^2$,[10] NO_2,$CONR^1R^2$,[11] or observed together with the amides in solution in these cases and in low concentrations in other cases such as when Y,Y′ = CO_2R,NO_2[8] or SO_2R,CO_2R.[12] When Y ≠ Y′, *E*- and *Z*-enols are frequently observed and their relative stabilities are determined to a significant extent by intramolecular hydrogen bonding to the enol hydrogen. K_{enol} values were measured for many enols as a function of Y,Y′, the amido *N*-substituents and the solvent, and NMR spectra serve as important probe in the structure assignment.

The present work investigates the possibility of generating enols when Y,Y′ are two dialkoxyphosphinyl $(RO)_2P{=}O$ groups or a combination of $(RO)_2P{=}O$ and CO_2R or CN. There are literature cases of enol formation activated by the presence of dialkoxyphosphinyl groups, but these are enols of aldehydes and ketones and not of carboxylic acids.[13,14] We are interested in the activating effect for enol formation and in hydrogen bonding ability of phosphonate vs ester group, and we want to compare the dialkoxyphosphinyl-substituted systems with di-esters like **E-3** and **Z-3**[5,7a,b] or with the cyanoesters **Z-4**.[7a,b,8] These systems showed a systematic behavior related to K_{enol} values, δ(OH) and δ(NH) values, the *E*/*Z* ratios, and the solid-state structures, with the increase in the number of fluorine atoms in the ester group(s). We want to find out if these features are also reflected in dialkoxyphosphinyl ester activated systems.

$HO(RR'N)C{=}C(CO_2R^1)CO_2R^2$ $HO(RR'N)C{=}C(CN)CO_2R^1$

E- and **Z-3**: R^1 = Me; R^2 = CF_3CH_2, $(CF_3)_2CH$ **Z-4**: R^1 = Me, CF_3CH_2, $(CF_3)_2CH$

Results and Discussion

Synthesis. Four groups (a−d) of "formal"[15] amido phosphonate systems had been prepared by the general method used previously for obtaining amides activated by Y, Y′.[4,5,7−10]

(a) Reactions of 2,2,2-trifluoroethyl or 1,1,1,3,3,3-hexafluoro-2-propyl chloroacetate (obtained from chloroacetyl chloride with 2,2,2-trifluoroethanol or with 1,1,1,3,3,3-hexafluoro-2-propanol, respectively) with trimethyl phosphite gave the phosphonate esters **5b** and **5c**. The methyl ester **5a** is commercial. The three esters were converted to their conjugated bases with Na in THF or in ether, and each of the anions was reacted with three aromatic and two aliphatic isocyanates XNCO (X = *p*-An, Ph, C_6F_5, *i*-Pr, *t*-Bu) to give 15 of the formal amido phosphonate esters (eq 2). The actual structures are either the amides **6a**−**o** or the *E*,*Z*-enols **7a**−**o** or their mixtures which were determined by ^{1}H, ^{13}C, ^{19}F, and ^{31}P NMR spectra.

$ClCH_2COCl + ROH \xrightarrow[CH_2Cl_2]{Et_3N} ClCH_2CO_2R \xrightarrow[80\text{-}90°C\ 48\text{-}60h]{(MeO)_3P}$

$(MeO)_2P(=O)CH_2CO_2R \xrightarrow[2.\ XNCO,0°C]{1.\ Na/THF\ or\ Et_2O,\ 0°C}$

5a: R = Me
5b: R = CF_3CH_2
5c: R = $(CF_3)_2CH$

$(MeO)_2P(=O)CH(CO_2R)(CONHX) \rightleftharpoons (MeO)_2P(=O)C(CO_2R){=}C(OH)NHX$ (*E* or *Z*) (2)

6a: R = Me	X = *p*-An	**7a:** R = Me	X = *p*-An
6b: R = Me	X = Ph	**7b:** R = Me	X = Ph
6c: R = Me	X = C_6F_5	**7c:** R = Me	X = C_6F_5
6d: R = Me	X = *i*-Pr	**7d:** R = Me	X = *i*-Pr
6e: R = Me	X = *t*-Bu	**7e:** R = Me	X = *t*-Bu
6f: R = CF_3CH_2	X = *p*-An	**7f:** R = CF_3CH_2	X = *p*-An
6g: R = CF_3CH_2	X = Ph	**7g:** R = CF_3CH_2	X = Ph
6h: R = CF_3CH_2	X = C_6F_5	**7h:** R = CF_3CH_2	X = C_6F_5
6i: R = CF_3CH_2	X = *i*-Pr	**7i:** R = CF_3CH_2	X = *i*-Pr
6j: R = CF_3CH_2	X = *t*-Bu	**7j:** R = CF_3CH_2	X = *t*-Bu
6k: R = $(CF_3)_2CH$	X = *p*-An	**7k:** R = $(CF_3)_2CH$	X = *p*-An
6l: R = $(CF_3)_2CH$	X = Ph	**7l:** R = $(CF_3)_2CH$	X = Ph
6m: R = $(CF_3)_2CH$	X = C_6F_5	**7m:** R = $(CF_3)_2CH$	X = C_6F_5
6n: R = $(CF_3)_2CH$	X = *i*-Pr	**7n:** R = $(CF_3)_2CH$	X = *i*-Pr
6o: R = $(CF_3)_2CH$	X = *t*-Bu	**7o:** R = $(CF_3)_2CH$	X = *t*-Bu

(b) By reacting chloroacetonitrile with trimethyl phosphite the dimethoxyphosphinylacetonitrile **8** was obtained, and reaction with Na, followed by reaction with XNCO (X = *p*-An, Ph, C_6F_5, *t*-Bu) gave the corresponding formal cyanoamidophosphonates which can be the amides **9a**−**d** or the enols **10a**−**d** (eq 3).

(2) Frey, J.; Rappoport, Z. *J. Am. Chem. Soc.* **1996**, *118*, 3994.
(3) Rappoport, Z.; Frey, J.; Sigalov, M.; Rochlin, E. *Pure Appl. Chem.* **1997**, *69*, 1933.
(4) Mukhopadhyaya, J. K.; Sklenak, S.; Rappoport, Z. *J. Am. Chem. Soc.* **2000**, *122*, 1325.
(5) Lei, Y. X.; Cerioni, G.; Rappoport, Z. *J. Org. Chem.* **2001**, *66*, 8379.
(6) Song, J.; Rappoport, Z. The 10th European Symposium on Organic Reactivity (ESOR 10), Rome, Italy, July 25−30, 2005, Abstract book, p 46.
(7) (a) Lei, Y. X.; Casarini, D.; Cerioni, G.; Rappoport, Z. *J. Org. Chem.* **2003**, *68*, 947. (b) Lei, Y. X.; Casarini, D.; Cerioni, G.; Rappoport, Z. *J. Phys. Org. Chem.* **2003**, *16*, 525. (c) Basheer, A.; Rappoport, Z. *J. Org. Chem.* **2004**, *69*, 1151.
(8) Mukhopadhyaya, J. K.; Sklenak, S.; Rappoport, Z. *J. Org. Chem.* **2000**, *65*, 6856.
(9) Basheer, A.; Yamataka, H.; Ammal, S. C.; Rappoport, Z. *J. Org. Chem.* **2007**, *72*, 5297.
(10) Basheer, A.; Rappoport, Z. Submitted for publication.
(11) (a) Simonsen, O.; Thorup, N. *Acta Crystallogr. Sect. B* **1979**, *57*, 1177. (b) Basheer, A.; Rappoport, Z. Unpublished results.
(12) Basheer, A.; Rappoport, Z. The 17th IUPAC Conference on Physical Organic Chemistry, Shanghai, China, August 15−20, 2004, Abstract IL-10, p 84.
(13) (a) Breuer, E. In *The Chemistry of Organophosphorus Compounds*; Hartley, F. R., Ed.; Wiley: Chichester, 1996; Vol. 4, Chapter 7, pp 694−698. (b) Afarinkia, K.; Echenique, J.; Nyburg, S. C. *Tetrahedron Lett.* **1997**, *38*, 1663.
(14) There are slightly related phosphato-substituted enols in biological systems such as phosphoenol pyruvate (Richard, J. P. In *The Chemistry of Enols*; Rappoport, Z., Ed.; Wiley: Chichester, 1990; Chapter 11).
(15) We use the term "formal" since in solution the compounds exist an amide/enols (*E* and *Z*) mixtures and in the solid state they may have an amide or an enol structure.

$$ClCH_2CN \xrightarrow[80\text{-}90°C\ 48\text{-}60h]{(MeO)_3P} (MeO)_2P(=O)CH_2CN \xrightarrow[2.\ XNCO,0°C]{1.\ Na/THF,\ 0°C} \underset{\mathbf{8}}{}$$

$$(MeO)_2P(=O)CHCN(CONHX) \rightleftharpoons (MeO)_2P(=O)C(CN)=C(OH)NHX \quad (3)$$

9a: X = *p*-An
9b: X = Ph
9c: X = C_6F_5
9d: X = *t*-Bu

10a: X = *p*-An
10b: X = Ph
10c: X = C_6F_5
10d: X = *t*-Bu

(c) Similarly to the reaction of group (a) above, reaction of the methylenebisphosphonate **11** with the five isocyanates gave five formal bisphosphonate amides which could be either the amides **12a**−**e** or the enols **13a**−**e** (eq 4).

$$\underset{\mathbf{11}}{[(MeO)_2P(=O)]_2CH_2} \xrightarrow[2.\ XNCO,0°C]{1.\ Na/THF,\ 0°C}$$

$$[(MeO)_2P(=O)]_2CH(CONHX) \rightleftharpoons [(MeO)_2P(=O)]_2C=C(OH)NHX \quad (4)$$

12a: X = *p*-An
12b: X = Ph
12c: X = C_6F_5
12d: X = *i*-Pr
12e: X = *t*-Bu

13a: X = *p*-An
13b: X = Ph
13c: X = C_6F_5
13d: X = *i*-Pr
13e: X = *t*-Bu

(d) When commercial methyl bis(trifluoroethoxy)phosphinylacetate **15** was refluxed with excess trifluoroethanol and catalytic amount of H_2SO_4, the methyl ester group was exchanged by a trifluoroethyl group to form the trifluoroethyl bis(trifluoroethoxy)phosphinylacetate **16**. Reaction of **15** or **16** with Na in ether, followed by reaction with the *p*-An, Ph, *i*-Pr, and *t*-Bu isocyanates, gave the eight formal bis(trifluoroethoxy)-phosphinyl amidoesters **17a**−**h** or their enols **18a**−**h** (eq 5).

$$\underset{\mathbf{15}}{(CF_3CH_2O)_2P(=O)CH_2CO_2Me} + CF_3CH_2OH\ (excess) \xrightarrow[reflux]{H_2SO_4}$$

$$\underset{\mathbf{16}}{(CF_3CH_2O)_2P(=O)CH_2CO_2CH_2CF_3}$$

$$(CF_3CH_2O)_2P(=O)CH_2CO_2R \xrightarrow[0°C]{Na/Et_2O} \xrightarrow[0°C]{XNCO} (CF_3CH_2O)_2P(=O)CH(CO_2R)CONHX \rightleftharpoons (CF_3CH_2O)_2P(=O)C(CO_2R)=C(OH)NHX \quad (5)$$

(E/Z)

17a: R = Me, X = *p*-An
17b: R = Me, X = Ph
17c: R = Me, X = *i*-Pr
17d: R = Me, X = *t*-Bu
17e: R = CF_3CH_2, X = *p*-An
17f: R = CF_3CH_2, X = Ph
17g: R = CF_3CH_2, X = *i*-Pr
17h: R = CF_3CH_2, X = *t*-Bu

18a: R = Me, X = *p*-An
18b: R = Me, X = Ph
18c: R = Me, X = *i*-Pr
18d: R = Me, X = *t*-Bu
18e: R = CF_3CH_2, X = *p*-An
18f: R = CF_3CH_2, X = Ph
18g: R = CF_3CH_2, X = *i*-Pr
18h: R = CF_3CH_2, X = *t*-Bu

All 31 amidophosphonates except **9b**[16] are new compounds.

The O═P(OMe)$_2$-substituted derivatives are not very stable. The fluoro derivatives frequently decompose during crystallization from 1:5−10 EtOAc−petroleum ether mixtures even at ca. −20 °C. X-ray crystallography showed that the decomposition product of **6f/7f** is **19** and that of **6m/7m** is **20**; i.e., the fluorinated ester moiety was lost during the crystallization. The crystallographic data of **19** and **20** (CIF) are provided in the Supporting Information.

$(MeO)_2P(=O)CH_2CONHAr$

19: Ar = *p*-An

20: Ar = C_6F_5

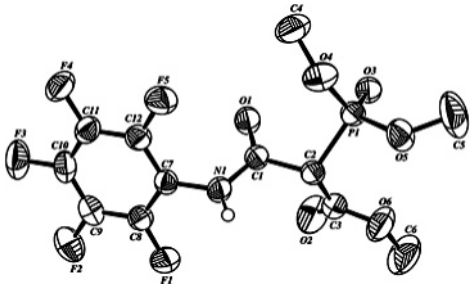

FIGURE 1. ORTEP drawing of the amide **6c**.

Solid-State Structures. We were able to obtain suitable crystals for X-ray diffraction of six of the amidophosphonates: four belonging to series (a), one to series (c), and one to series (d). We failed in obtaining suitable crystals in the cyano series (b).

In series (a), we determined the solid-state structures of **6c/7c** with no fluorine atoms in the ester group, of **6g/7g** having three fluorine atoms in the ester group, and of **6k/7k** and **6n/7n**, both having six fluorine atoms in the ester group. The ORTEP drawing of **6c** and **7k** are given in Figures 1 and 2, respectively, and selected crystallographic parameters of the four compounds are given in Table 1. Other ORTEPs and the full crystallographic parameters are given in the Supporting Information.

The structures of the first two compounds with none or three fluorines in the ester groups are those of the amides **6c** and **6g**. Their bond lengths and angles, except for one bond length and one angle, are identical within the experimental error, with normal C−C and C−N bond lengths, while the short bonds of 1.18 and 1.21 Å are characteristic of a C═O of a C(C═O)X moiety.[17]

In contrast, the hexafluoroester derivatives display the enol structures **7k** and **7n**. The data for both compounds are in Table 1. Characteristic important features for Y,Y′-activated enols are the elongated C(1)−C(2) bond, compared with a normal C═C value, of 1.337 to 1.41−1.42 Å (indicating a dipolar structure) which is only 0.01 Å shorter than the C(2)−C(3) bond and the conversion of the amido C═O to a single C−O bond of 1.313−1.321 Å, whereas the ester C═O bond length remains 1.21 ± 0.004 Å. The angles around the C(1)−C(2) bond are mostly around 120°. For compound **7k** there are three independent molecules in the unit cell. In two of them the N-*p*-An group and the C═C bond are nearly coplanar, whereas they are nearly perpendicular in the third molecule. Almost all parameters involving heavy atoms are nearly the same.

The enol can have an *E* or *Z*-configuration. The enolic OH was found to be cis to the O═P(OMe)$_2$ group, rather than to the $CO_2CH(CF_3)_2$ in both enols. The nonbonded O(1)···O(3) distances of 2.488−2.513 Å indicate a moderate to strong O−H···O═P hydrogen bond. This resembles the configuration in enols **3**, $R^2 = (CF_3)_2CH$, where the hydrogen bonding is *not* to the $CO_2CH(CF_3)_2$ group.[5]

The hydrogen bond is asymmetric with O(1)−H and O(3)···H bond lengths or distances of 1.02(6) and 1.54(6)Å in **7n** and 1.00(4) and 1.52 Å for one molecule of **7k**, i.e., Δ_{OH} = 0.52 Å. However, Δ_{OH} values are 0.68 and 0.74 Å in the other two independent molecules of **7k**. This may reflect the difficulty in locating hydrogens in the X-ray diffraction. The O(1)HO(3) angles are 158(4)−162(4)°; i.e., the hydrogen bond is not far from being linear.

(16) Hamlet, Z.; Mychajlowskij, W. *Chem. Ind. (London, UK)* **1974**, (20), 829.

(17) Allen, F. H.; Kennard, O.; Watson, D. G.; Brammer, L.; Orpen, A. G.; Taylor, R. *J. Chem. Soc., Perkin Trans. 2* **1987**, S1.

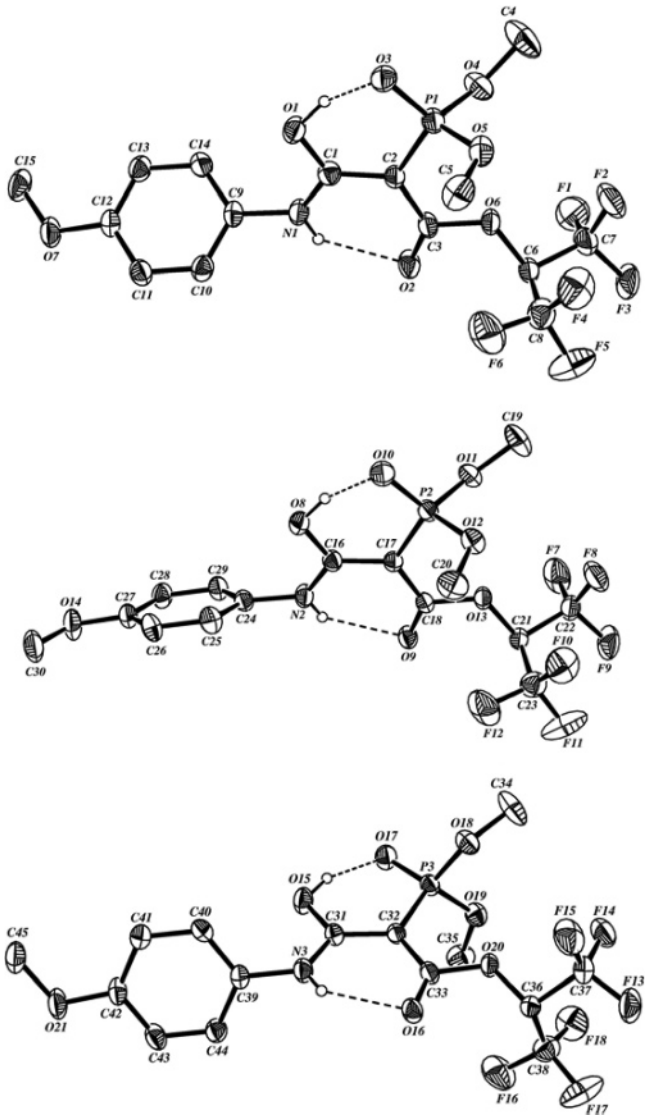

FIGURE 2. ORTEP drawing of the enol **7k**.

Similarly to the diester activated systems, there is an additional N−H···O═C hydrogen bond to the ester group, with an N···O nonbonding distances of 2.695(4)−2.726(3) Å, N−H and O···H distances of 0.72(3)−0.82(4) and 2.00(4)−2.11(3) Å, and an N(1)HO(2) angles of 131(3)−142(4)°.

The structural change from an ester carrying 0 to 3 and then 6 fluorine atoms resembles the finding for the solid diester systems, where the structure is that of an amide with 0 and 3 fluorines, but an enol for the 6-F compounds. In both cases the activation for enol formation increases, but the hydrogen bond accepting ability decreases with the increased electron-withdrawal by the ester group.

Structure in Solution. The probes for the structure(s) and compositions of the mixtures in solution were ^{1}H, ^{13}C, ^{19}F, and ^{31}P NMR spectra which were recorded for all systems in five solvents of different polarity: CCl_4, $CDCl_3$, THF-d_8, CD_3CN, and DMSO-d_6, mostly at 298 K and occasionally at lower temperatures. All spectra were used for qualitative structural analysis, whereas ^{1}H, ^{19}F, and ^{31}P spectra were also used for quantitative determination of the compositions of the various species in solution which were structure and solvent dependent.

The ^{1}H NMR δ(OH) and δ(NH) and δ(CH) values for the enols and the amides are given in Table 2. It is noteworthy that for the amide the hydrogens of the OCH_3 of **6** and the CH_2 hydrogens of the OCH_2CF_3 on P of **17** appear as two doublets, each one with $^{3}J_{PH}$ = ca. 11.5 Hz. This is ascribed to two diastereotopic signals due to the chiral center. In ca. 15% of the cases only one doublet was observed and this is attributed to overlap of the two doublets. Two doublets appear also for the carbons bearing these hydrogens (see below).

The full data are given in Table S1 in the Supporting Information.

Selected ^{13}C, ^{19}F, and ^{31}P NMR data are given in Tables 3 and 4. The full data are given in Tables S2 and S3 in the Supporting Information. In all cases, small unidentified signals or signals due to decomposition are omitted.

^{1}H NMR. Table 2 gives the lowest field ^{1}H NMR range which includes the OH and NH signals of the enols and amides and the higher field CH signals of the amides. For series (a) and (d) there are two sets of signals with δ >8.40 ppm in CCl_4, $CDCl_3$, THF-d_8, and CD_3CN (except for **7c**, **7g**, and **7h** for which few OH signals in some solvents were not observed, perhaps due to fast intermolecular exchange), but none in DMSO-d_6. The lowest field set is at δ 12.92−16.84, and the higher field set is at δ 8.40−12.00, and the values change systematically depending on the nitrogen-X and the ester-R substituents. Each signal in each group has a signal with identical integration in the other group and by comparison with the integration of the methyls of the *p*-anisyl, *i*-Pr, or *t*-Bu groups, these signals are identified as one hydrogen signals. In parallel with previously studied enol systems,[4−10] they were identified as the enol of amide OH (at the lowest field) and NH (at the higher field) signals. Moreover, in parallel with systems ***E*-3/*Z*-3**[5] the two signals in each groups belong to the *E* and *Z* isomers. As with enols ***E*-3/*Z*-3**, the OH signal at the lowest field for **7a**−**e** belong to the same enol with the highest field NH signal, whereas the "internal" signals between them belong to the other isomer. The other two signals in Table 2 at a higher field have similar integration in each species and are the NH (at δ 6.42−10.54) and the CH (at δ 3.47−5.09) of the amide. The latter is easily identified since the proton is split to a doublet by the phosphorus.

Inspection of Table 2 leads to several generalizations. (a) The lowest field OH and NH signals are consistently in THF-d_8. The order of the four signals as a function of the solvent at 298 K is THF-d_8 > CD_3CN > $CDCl_3$ > CCl_4, and the differences between the extreme δ values, e.g., for δ(OH) of the *E*-enol, are 0.42−0.65 ppm for the **6**/**7** series. Data for the other signals and for the **17**/**18** series are given in Table 5a. (b) The *N*-aryl substituent effect in the **6**/**7** series is not systematic. An increase in the electron-donating ability of the aryl ring results in the order *p*-An < Ph > C_6F_5 for δ(OH,*E*-enol), whereas for δ-(OH,*Z*-enol) the order is *p*-An < Ph < C_6F_5. In the **17**/**18** systems the order is *p*-An < Ph. For *N*-aliphatic substituents δ(OH) and δ(NH) values follow the order *i*-Pr < *t*-Bu. These δ values for the *N*-alkyl substituents are always lower than for the aromatic ones both in the **6**/**7** and **17**/**18** systems, with more significant differences for the δ(NH) in the **6**/**7** series.

(c) The mechanistically most revealing data are the differences due to the change of the ester group R within the series **6**/**7** and **17**/**18**. All of the following quoted differences are for the same solvent and *N*-substituent. The differences between members of the **7a**−**e** (R = CO_2Me) and the **7f**−**j** (R = CF_3CH_2) series

TABLE 1. Selected X-ray Data for 7n, 7k, 6g, and 6c at Room Temperature

	length, Å			
bond	**7n**	**7k**	**6g**	**6c**
C(1)−C(2)	1.418(5)	1.414(4) [1.420(4)] (1.416(4))	1.537(5)	1.524(2)
C(1)−N(1)	1.306(5)	1.306(4) [1.311(4)] (1.314(4))	1.336(5)	1.352(2)
C(1)−O(1)	1.318(5)	1.321(4) [1.316(3)] (1.313(3))	1.217(5)	1.213(2)
C(2)−C(3)	1.426(5)	1.427(4) [1.427(4)] (1.423(4))	1.519(5)	1.524(3)
C(2)−P(1)	1.754(3)	1.751(3) [1.752(3)] (1.755(3))	1.810(4)	1.8162(18)
C(3)−O(2)	1.213(4)	1.206(4) [1.208(3)] (1.206(3))	1.183(5)	1.180(3)
C(3)−O(6)	1.375(4)	1.393(3) [1.387(3)] (1.384(3))	1.333(5)	1.311(3)
O(3)−P(1)	1.484(3)	1.487(2) [1.484(2)] (1.485(2))	1.449(3)	1.4654(14)
O(1)−H	1.02(6)	1.00(4) [0.93(4)] (0.90(4))		
O(3)−H	1.54(6)	1.52(4) [1.61(4)] (1.64(5))		
O(1)−O(3)	2.513(4)	2.488(3) [2.502(3)] (2.500(3))		
N(1)−H	0.82(4)	0.85(3) [0.76(3)] (0.72(3))		
O(2)−H	2.00(4)	2.08(3) [2.11(3)] (2.10(3))		
N(1)−O(2)	2.695(4)	2.716(3) [2.726(3)] (2.709(3))		
	angle (deg)			
bond angle	**7n**	**7k**	**6g**	**6c**
N(1)C(1)O(1)	114.9(4)	114.7(3) [114.2(3)] (114.5(3))	125.2(4)	123.73(17)
N(1)C(1)C(2)	123.2(3)	123.6(3) [124.0(3)] (123.5(3))	114.6(4)	113.89(15)
O(1)C(1)C(2)	121.9(3)	121.7(3) [121.7(3)] (122.0(3))	120.2(3)	122.38(16)
C(1)C(2)C(3)	119.4(3)	119.1(3) [119.2(3)] (119.4(3))	110.6(3)	109.61(15)
C(1)C(2)P(1)	119.3(3)	119.1(2) [119.3(2)] (119.0(2))	109.6(2)	110.11(12)
C(3)C(2)P(1)	121.3(3)	121.8(2) [121.6(2)] (121.7(2))	111.0(3)	111.50(13)
O(2)C(3)C(2)	128.4(3)	129.7(3) [129.2(3)] (129.1(3))	126.1(4)	124.54(19)
O(2)C(3)O(6)	120.5(3)	120.3(3) [120.5(3)] (120.6(3))	124.2(4)	124.8(2)
O(6)C(3)C(2)	111.2(3)	110.0(3) [110.3(3)] (110.4(2))	109.7(3)	110.63(18)
O(1)HO(3)	159(5)	161(4) [162(4)] (158(4))		
N(1)HO(2)	142(4)	131(3) [138(3)] (142(3))		

are nearly constant. For the δ(OH,*E*-enol) they are 0.95−1.09 ppm for the aromatic substituents. There are differences in the values for *N*-Ar and *N*-Alk substituents and the average values, as well as the other signals discussed below are given in Table 5b. The differences between the **7f**−**j** (R = CF_3CH_2) series and the **7k**−**o** (R = $(CF_3)_2CH$) series are also approximately constant, being 0.76−1.01 ppm. For the δ(OH, *Z*-enol) the differences between the **7a**−**e** and **7f**−**j** series are negative, being −0.16 to −0.27 ppm, and the differences between the **7f**−**j** and **7k**−**o** series show a large variation of −0.07 to −0.28 ppm.

For the δ(NH,*E*-enol) signals, the differences between the **7a**−**e** and the **7f**−**j** series are also negative , being −0.16 to −0.27 ppm, and the differences between the **7f**−**j** and **7k**−**o** series are −0.11 to −0.24 ppm. For the δ(NH,*Z*-enol), the differences between the **7a**−**e** and **7f**−**j** series are positive, being 0.20−0.37 ppm, and the differences between the **7f**−**j** and **7k**−**o** series are 0.15−0.32 ppm.

(d) The $\Delta\delta$(OH)(*E*-enol − *Z*-enol) values for the **7a**−**e** (R = Me) pairs also depend on the *N*-substituents, being 1.51−1.83 ppm. Values for the *N*-Ar and *N*-Alk subgroups for these and other systems and signals are given in Table 5c. For **7f**−**j** (R = CF_3CH_2), the differences are much smaller: 0.27−0.76 ppm. For **7k**−**o** (R = $(CF_3)_2CH$), the values are negative, being −0.20 to −1.11 ppm.

The $\Delta\delta$(NH)(*E*-enol − *Z*-enol) differences for **6**/**7**(R = Me) are negative , −0.09 − −0.44 ppm. When R = CF_3CH_2 the values are positive, being 0.06−0.54. When R = $(CF_3)_2CH$ the values are more positive, being 0.44−1.02 ppm. Table 5c gives the smaller ranges for the sub-groups.

(e) Electron withdrawal from the phosphorus for the **18a**−**h** system carrying $(CF_3CH_2O)_2$ groups was probed by comparison with the corresponding **7a**,**b**,**d**−**g**,**i**,**j** systems carrying $(MeO)_2$ groups (Table 5d). Remarkably, the differences between systems **7** and **18** for the δ(OH,*E*-enol) and the δ(NH,*Z*-enol) were very small, being 0.02−0.23 (average for 27 pairs 0.12 ± 0.05) and −0.13 to +0.03 (average for 32 pairs −0.03 ± 0.04), respectively. The largest difference is for δ(OH,*Z*-enol) where the values for series **7** are 0.84−1.14 ppm higher than for system **18** when R = Me and 0.92−1.21 ppm when R = CF_3CH_2. The δ(NH,*E*-enol) is also higher for system **7** than for **18** by 0.18 −0.61 ppm when R = Me and by 0.38−0.60 ppm when R = CF_3CH_2 (Table 5d).

$\Delta\delta$(OH)(*E*-enol − *Z*-enol) values for **18** are 2.33−2.67 when R = Me (average 2.53 ± 0.10). When R = CF_3CH_2, the range is 1.21−1.58 (average 1.42 ± 0.08). The $\Delta\delta$(NH)(*E*-enol − *Z*-enol) values are negative: −0.63 to −0.94 ppm when R = Me (average 0.77 ± 0.10 ppm) and −0.14 to −0.46 ppm when R = CF_3CH_2 (average −0.29 ± 0.10 ppm) (Table 5c).

(f) For seven and eight compounds, δ(OH) and δ(NH) values were determined also at 240 K in addition to 298 K. The temperature effect depends on the isomer and the signal. In series **7**, the values in ppm are as follows: *E*-enol OH +0.03 to −0.16 (average −0.04 ± 0.03), *Z*-enol OH 0.04−0.19 (average 0.10 ± 0.02), *E*-enol NH 0.06−0.17 (average 0.11 ± 0.03), and *Z*-enol NH −0.03 to +0.05 (average −0.01 ± 0.01). For the cyano enols **10** the *E*-enol OH signal was not observed at all, and it was observed only at 240 K for the *Z*-enol OH. For **10d** it decreased by 0.08 ppm from 298 to 240 K. In contrast, the δ(NH) signals were observed at both temperatures, and the temperature effect was significantly larger than in series **7** for seven of the eight values. δ(NH) for the *Z*-enol increase at 240 K by 0.51, 0.59, 0.68, and 0.08 ppm and for the amide by 0.76, 0.66, 0.90, and 0.38 ppm. A similar 298K → 240K change in CD_3CN was small: −0.02 ± 0.04, −0.08 ± 0.02, −0.08 ±

TABLE 2. Relevant ^{1}H NMR Data for All Enol/Amide Systems in Five Solvents at 298 K

		δ_{OH}, ppm		δ_{NH}, ppm		δ_{NH}, ppm	δ_{CH},[a] ppm
compd	solvent	*E*-enol	*Z*-enol	*E*-enol	*Z*-enol	amide	amide
6a/7a	CCl_4	16.03	14.44 (br)	10.93	11.22	8.59	3.64
	$CDCl_3$	16.35	14.57	11.02	11.46	9.05	4.22
	THF-d_8	16.63	15.10	11.53	11.62	9.23	4.26
	CD_3CN	16.49	14.85	11.26	11.42	8.84	4.28
	DMSO-d_6					10.09	4.51
6b/7b	CCl_4	16.19	14.58	11.12	11.39	8.77	3.72
	$CDCl_3$	16.49	14.72	11.30	11.63	9.13	4.21
	$CDCl_3$ (240 K)	16.53	14.65	11.24	11.64	9.40	4.33
	THF-d_8	16.84	15.20	11.73	11.80	9.38	4.31
	CD_3CN	16.63	15.00	11.47	11.62	8.98	4.31
	DMSO-d_6					10.23	4.57
6c/7c	CCl_4	16.11	14.60 (br)	10.70	10.82	8.62	3.80
	$CDCl_3$	16.45		10.86	11.09	8.96	4.30
	THF-d_8	16.70		11.09	11.20	9.30	4.42
	CD_3CN					8.76	4.41
	DMSO-d_6					10.35	4.71
6d/7d	CCl_4	15.52	13.90	8.89	9.20	6.61	3.51
	$CDCl_3$	15.77	14.00	9.12	9.46	7.00	4.01
	THF-d_8	16.10	14.59	9.50	9.63	7.16	4.03
	CD_3CN	16.02	14.36	9.28	9.53	6.88	4.04
	DMSO-d_6					7.93	4.27
6e/7e	CCl_4	15.69	13.98	9.07	9.45	6.64	3.47
	$CDCl_3$	15.89	14.06	9.33	9.75	7.07	3.99
	THF-d_8	16.27	14.68	9.71	9.90	7.11	3.98
	CD_3CN	16.15	14.43	9.51	9.80	6.84	3.99
	DMSO-d_6					7.67	4.34
6f/7f	CCl_4	15.03	14.64	11.14	10.86	8.53	3.77
	$CDCl_3$	15.38	14.78 (br)	11.29	11.15	8.88	4.31
	THF-d_8	15.54	15.27	11.69	11.26	9.18	4.43
	CD_3CN	15.45	15.02	11.42	11.10	8.74	4.41
	CD_3CN (255 K)	15.47	14.94	11.36	11.08	9.00	4.47
	DMSO-d_6					10.15	4.68
6g/7g	CCl_4	15.18	14.81	11.28	11.02	8.86	3.99
	$CDCl_3$	15.52	14.94 (br)	11.53	11.32	9.05	4.36
	$CDCl_3$ (240 K)	15.58	14.90	11.43	11.35	9.33	ov
	THF-d_8	15.79	15.47	11.87	11.44	9.38	4.52
	CD_3CN			11.62	11.28	8.92	4.46
	CD_3CN(240K)	15.66	15.14	11.57	11.29	9.25	4.55
	DMSO-d_6					10.29	4.74
6h/7h	CCl_4	15.01		10.88	10.40	8.71	4.03
	$CDCl_3$	15.39		11.06	10.75	8.89	4.43
	$CDCl_3$ (240 K)	15.55	14.98	10.93	10.75	9.39	ov
	THF-d_8			11.37	10.76	9.33	ov
	THF-d_8 (240 K)	15.75	15.60	11.25	10.81	9.71	4.79
	CD_3CN	15.56		11.19	10.65	8.68	4.57
	DMSO-d_6					10.45	4.89
6i/7i	CCl_4	14.60	14.14	9.10	8.90	6.64	ov
	$CDCl_3$	14.88	14.20	9.30	9.20	6.90	4.11
	THF-d_8	15.16	14.76	9.68	9.34	7.19	4.22
	CD_3CN	15.07	14.52	9.47	9.28	6.91	4.22
	DMSO-d_6		14.64		9.29	8.01	4.44
6j/7j	CCl_4	14.78	14.23	9.30	9.15	6.63	3.64
	$CDCl_3$	15.03 (t)	14.27 (br)	9.54	9.48	6.92	4.07
	$CDCl_3$ (240 K)	15.00	14.18	9.47	9.49	7.04	4.16
	THF-d_8	15.34	14.88	9.92	9.62	7.09	4.17
	CD_3CN	15.21	14.62	9.72	9.53	6.76	4.13
	CD_3CN (240 K)	15.24	14.55	9.63	9.56	6.92	4.18
	DMSO-d_6		14.70		9.54	7.79	4.51
6k/7k	CCl_4	14.27	14.81	11.25	10.59	8.41	*b*
	$CDCl_3$	14.62	14.95 (br)	11.43	10.91	8.82	4.38
	THF-d_8	14.71	15.33 (br)	11.81	10.96	9.24	4.64
	CD_3CN	14.55	15.15	11.60	10.82	8.71	4.55
	CD_3CN (240 K)	14.48	15.03	11.49	10.75	8.98	4.61
	DMSO-d_6				10.85	10.21	4.84
6l/7l	CCl_4	14.40	15.03	11.43	10.73	8.79	4.07
	$CDCl_3$	14.75	15.12	11.59	11.07	8.73	4.42
	$CDCl_3$ (240 K)	14.79	14.99	11.46	11.08	9.22	4.58
	THF-d_8	14.87	15.54	12.00	11.12	9.39	4.69
	CD_3CN	14.66	15.32 (br)	11.76	10.97	8.85	4.59
	DMSO-d_6					10.34	4.90
6m/6m	CCl_4	14.23	15.30 (br)	11.11	10.11	8.61	4.13
	$CDCl_3$	14.60	15.34 (br)	11.26	10.47	8.79	4.53
	$CDCl_3$ (240 K)	14.61	15.26	11.14	10.50	9.73	4.76
	THF-d_8	14.65	15.76	11.53	10.51	9.37	4.86
	CD_3CN	14.55	15.60	11.34	10.35	8.64	4.75
	DMSO-d_6					10.54	5.09

Table 2 (Continued)

		δ_{OH}, ppm		δ_{NH}, ppm		δ_{NH}, ppm	δ_{CH},[a] ppm
compd	solvent	*E*-enol	*Z*-enol	*E*-enol	*Z*-enol	amide	amide
6n/7n	CCl_4	13.91	14.36	9.29	8.70	*b*	*b*
	$CDCl_3$	14.22	14.42	9.54	9.05	6.87	4.20
	$CDCl_3$ (240 K)	14.20	14.29	9.41	9.05	7.03	4.31
	THF-d_8	14.37	14.95	9.91	9.12	7.24	4.38
	CD_3CN	14.22	14.69	9.65	9.04	6.79	4.32
	DMSO-d_6		14.64		9.11	8.11	4.61
6o/7o	CCl_4	14.07	14.44	9.50	8.93	*b*	*b*
	$CDCl_3$	14.34	14.45	9.72	9.28	6.87	4.13
	$CDCl_3$ (240 K)	overlap Z-enol	14.26	9.55	9.23	6.95	4.19
	THF-d_8	14.53	15.03	10.10	9.38	7.13	4.37
	THF-d_8 (240 K)	14.88	15.06	9.89	9.28	7.47	4.45
	CD_3CN	14.35	14.75	9.89	9.28	6.76	4.29
	CD_3CN (255 K)	14.32	14.70	9.83	9.28	6.82	4.36
	DMSO-d_6		14.73		9.34	7.90	4.68
9a/10a	$CDCl_3$				7.58	8.83	4.33
	$CDCl_3$ (240 K)		13.34		8.09	9.59	4.57
9b/10b	$CDCl_3$				7.92	9.12	4.46
	$CDCl_3$ (240 K)		13.45		8.51	9.78	4.64
9c/10c	$CDCl_3$				7.98	9.01	4.45
	$CDCl_3$ (240 K)				8.66	9.91	4.65
9d/10d	$CDCl_3$		13.07		5.58	6.53	3.98
	$CDCl_3$ (240 K)		12.99		5.66	6.91	4.17
12a/13a	$CDCl_3$					8.78	3.79
12b/13b	$CDCl_3$					9.04	3.91
12c/13c	$CDCl_3$					8.84	3.98
12d/13d	$CDCl_3$					6.67	3.56
12e/13e	$CDCl_3$					6.66	3.47
17a/18a	CCl_4	15.95	13.30	10.34	11.22	8.52	ov
	$CDCl_3$	16.21	13.57	10.59	11.44	8.82	4.39
	THF-d_8	16.47 (br)	14.03 (br)	10.96	11.59	9.28	4.45
	CD_3CN			10.77	11.40	8.66	4.50
	DMSO-d_6					10.22/10.17	4.82
17b/18b	CCl_4	16.14	13.47 (br)	10.51	11.39	8.74	3.97
	$CDCl_3$	16.39	13.73 (br)	10.77	11.62	8.96	4.36
	THF-d_8			11.15	11.78	9.52	4.65
	CD_3CN			10.96	11.60	8.84	4.56
	DMSO-d_6					10.38	4.88
17c/18c	CCl_4	15.46 (t)	12.92	8.40	9.28	6.42	ov
	$CDCl_3$	15.67 (t)	13.16	8.72 (d)	9.56 (d)	6.75 (d)	4.19
	THF-d_8	15.95	13.62	9.01	9.68	7.25 (d)	4.31
	CD_3CN	15.79	13.41	8.90	9.57	6.72	4.26
	DMSO-d_6					8.11/8.03 (d)	4.58
17d/18d	CCl_4	15.63	13.00	8.59	9.53	6.47	3.65
	$CDCl_3$	15.75	13.19	8.89	9.77	6.73	4.10
	THF-d_8	16.12	13.71	9.22	9.94	7.09	4.29
	CD_3CN	15.94 (br)	13.46 (br)	9.13	9.85	6.63	4.23
	DMSO-d_6					7.87	4.64
17e/18e	CCl_4	14.99	13.53	10.57	10.92	8.48	ov
	$CDCl_3$	15.24	13.70	10.75	11.15	8.45	ov
	THF-d_8	15.40	14.19	11.09	11.25	9.32	4.65
	CD_3CN	15.28	13.94	10.91	11.08	8.61	4.60
	DMSO-d_6					10.29	4.97
17f/18f	CCl_4	15.16	13.70	10.74	11.08	8.28	ov
	$CDCl_3$	15.39	13.86	10.93	11.31	8.62	ov
	THF-d_8	15.64	14.26 (br)	11.28	11.42	9.45	4.69
	CD_3CN	15.38	14.09	11.10	11.26	8.75	4.64
	DMSO-d_6					10.42	5.03
17g/18g	CCl_4	14.55	13.14	8.65 (d)	9.01 (d)	*b*	*b*
	$CDCl_3$	14.78	13.28	8.89	9.29	6.48	ov
	THF-d_8	15.05	13.76	9.22	9.41	7.32 (d)	ov
	CD_3CN	14.92	13.54	9.09	9.31	6.71	4.37
	DMSO-d_6				9.16 (br)	8.20 (d)	4.74
17h/18h	CCl_4	14.74	13.23	8.85	9.28	6.71	ov
	$CDCl_3$	14.90	13.32	9.06	9.52	6.47	ov
	THF-d_8	15.21	13.84	9.42	9.67	7.19	4.46
	CD_3CN	15.01	13.59	9.27	9.56	6.62	4.36
	DMSO-d_6					7.97	4.80

[a] ov: overlaps another signal. [b] The signal is too weak to be observed.

0.02, and -0.01 ± 0.03 ppm for three or four cases for the *E*-enol OH, *Z*-enol OH, *E*-enol NH, and *Z*-enol NH, respectively. The magnitude of the temperature effect in THF-d_8 was larger, but only two compounds were studied.

TABLE 3. Selected ^{13}C NMR Data for Several Enol/Amide Systems in $CDCl_3$[a]

compd	solvent	*T* (K)	species	C_β	C_α	ACH_2O-PO[b]	CO_2R
6a/7a	$CDCl_3$	298	amide	54.2	158.7	54.4	166.2
6b/7b	$CDCl_3$	298	amide	54.41	158.9	54.42	166.2
6d/7d	$CDCl_3$	298	*E*-enol	60.4	172.0	52.3	174.7
			Z-enol	58.3	170.9	52.8	170.0
			amide		160.0	54.20, 54.13	166.1
6g/7g	$CDCl_3$	298	*E*-enol	61.81	171.9	52.69	172.4
			Z-enol	60.43	170.8	53.16	167.5
			amide	53.96	158.2	54.61, 54.54	164.0
6i/7i	$CDCl_3$	298	*E*-enol	60.85	170.93	52.32	172.09
			Z-enol	58.46	171.98	52.85	167.31
			amide	58.24	159.24	54.29, 54.22	163.92
6k/7k	$CDCl_3$	298	*E*-enol	62.4	171.2	52.70	170.1
			Z-enol	59.8	170.7	53.15	165.4
6l/7l	$CDCl_3$	298	*Z*-enol	60.24	170.93	53.20	165.46
6m/7m	$CDCl_3$	240	*E*-enol		173.2		169.9
			Z-enol	61.5	172.1	53.7	165.2
			amide		158.9		162.9
6n/7n	$CDCl_3$	240	*Z*-enol	57.57	170.17	53.16	164.91
9b/10b	$CDCl_3$	298	amide	39.2	156.4	55.4, 55.3	
9d/10d	$CDCl_3$	298	amide	39.2	156.9	55.4, 55.0	
12a/13a	$CDCl_3$	298	amide	48.3	158.5	54.3	
12c/13c	$CDCl_3$	298	amide	47.4	160.2	54.4	
12e/13e	$CDCl_3$	298	amide	48.3	159.4	54.0	
17a/18a	$CDCl_3$	298	*Z*-enol	59.57	169.79	63.20	169.14
			E-enol	61.16	171.59	62.41	174.39
			amide	54.44	157.78	63.47, 63.30	165.35
17e/18e	$CDCl_3$	298	*Z*-enol	59.89	169.86	62.86	166.80
			E-enol	61.81	171.14	62.52	171.82
			amide	54.18	158.20		162.44
17g/18g	$CDCl_3$	298	*Z*-enol	58.43	170.16	62.41	166.69
			E-enol	60.55	171.47	61.99	171.69
6j/7j	CCl_4	298	*E*-enol	61.4	172.8	51.5	171.83
			Z-enol	58.66	171.77	52.0	166.8
			amide	53.51	158.1	53.43	166.8
	$CDCl_3$	298	*E*-enol	61.3	173.0	52.45	172.3
			Z-enol	58.9	171.9	52.96	167.6
			amide	54.2	159.1	54.42, 54.29	164.1
	THF-d_8	298	*E*-enol	61.6	173.4	51.21	172.6
			Z-enol	58.7	172.3	51.92	167.2
			amide	53.65	159.4	53.18, 53.06	163.6
	DMSO-d_6	298	amide	53.2	160.6	54.1	163.8
6o/7o	CCl_4	298	*E*-enol	61.6	172.3	51.5	169.6
			Z-enol	58.6	171.7	52.1	164.8
	$CDCl_3$	240	*E*-enol	60.7	171.9	52.7	169.6
			Z-enol	58.0	171.1	53.1	165.1
	THF-d_8	240	*Z*-Enol	57.9	171.8	52.1	165.0
	CD_3CN	255	*Z*-enol	57.1	171.3	52.1	164.6
			amide	52.2	158.9	53.5, 53.4	161.8
	DMSO-d_6	298	*Z*-enol	58.6	171.8	52.9	163.8
			amide	52.8	159.9	54.2, 54.1	162.3
17d/18d	CCl_4	298	*E*-enol	59.89	172.74	61.60	173.84
			Z-enol	57.88	170.92	62.05	168.24
			amide	54.09	157.71	62.95, 62.51	165.04
	$CDCl_3$	298	*E*-enol	60.15	172.89	62.29	174.42
			Z-enol	58.31	171.10	62.73	169.34
			amide	54.83	158.63	63.40, 63.07	165.46
	THF-d_8	298	*E*-enol	60.58	173.27	61.68	174.66
			Z-enol	58.37	171.55	62.21	168.85
			amide	54.41	159.83	63.07, 62.84	164.62
	CD_3CN	298	amide	54.52	159.99	62.96, 62.72	164.86
	DMSO-d_6	298	amide	54.20	160.61	62.93, 62.67	164.91

[a] Some signals are missing due to too weak intensity or to a difficulty in identification. [b] A = H or CF_3.

(g) The range of the δ(NH) signal for the amides is mostly DMSO-d_6 ≫ THF-d_8 > $CDCl_3$ > CCl_4. In ppm for *N*-Ar compounds it is at 8.28−9.52 (in DMSO-d_6 10.09−10.54) and for *N*-alkyl compounds 6.42−7.47 (in DMSO-d_6 7.67 − 8.20).

How can the configuration of each group of species be deduced from these data? This was easy for series **3** and **4** where the orders of increased electron withdrawal of the ester R groups and the decreasing hydrogen bond accepting abilities were $(CF_3)_2CH$ > CF_3CH_2 > CH_3.[5,7] The values of δ(OH) and δ(NH) followed these values. In the present systems where O═P(OMe)$_2$ and O═P(OCH$_2$CF$_3$)$_2$ groups are present the changes in δ values are not monotonous, and hence, we present them in Table 2 according to the *E* and the *Z* species to which they belong, and the reasoning for this is given below.

The two geometric isomers to be considered are the *E* isomers (***E*-21**−***E*-25**) and the *Z* isomers (***Z*-21**−***Z*-25**). As in previous

TABLE 4. Selected ^{19}F and ^{31}P NMR Data of All Enol/Amide Systems at 298K

	^{19}F NMR in $CDCl_3$			^{31}P NMR in CCl_4		
compd	*E*-enol	*Z*-enol	amide	*E*-enol	*Z*-enol	amide
6a/7a				26.10	33.36	17.00
6b/7b				25.84	33.29	16.92
6c/7c				24.95	31.96	15.71
6d/7d				26.55	33.87	17.21
6e/7e				26.81	34.15	17.46
6f/7f	−74.81	−74.78	−74.41	24.05	31.47	16.3
6g/7g	−74.8	−74.77	−74.4	23.79	31.42	16.22
6h/7h	−74.85	−74.81	−74.52	22.94	30.29	15.34
6i/7i	−74.9	−74.87	−74.5	24.53	31.87	16.37
6j/7j	−74.89	−74.86	−74.48	24.64	32.12	15.60
6k/7k	−74.25		−73.81 (m)	22.62	30.09	15.57
6l/7l	−74.27		−73.85	22.33	30.07	15.43
6m/7m	−74.24		−73.87	21.52	29.17	14.90
6n/7n	−74.34		−73.89	22.89	30.38	15.69
6o/7o	−74.32		−73.88	23.06	30.66	16.00
9a/10a[a]						13.64
9b/10b[a]						13.34
9c/10c[a]						12.18
9d/10d[a]						14.19
12a/13a[a]						17.57
12b/13b[a]						17.43
12c/13c[a]						16.4
12d/13d[a]						17.81
12e/13e[a]						18.05
17a/18a[b]	−75.90	−75.88	−76.16	26.05	31.92	17.01
17b/18b[b]	−75.93	−75.91	−76.22	25.78	31.79	16.89
17c/18c[b]	−76.01	−75.98	−76.23/−76.24	26.50	32.41	17.14
17d/18d[b]	−75.94	−75.91	−76.16/−76.17	26.71	32.63	17.33
17e/18e[b]	−76.02	−76.00	−76.19	24.28	30.2	16.06
17f/18f[b]	−76.04	−76.01	−76.21	24.03	30.08	15.93
17g/18g[b]	−76.18	−76.13		24.64	30.61	16.20
17h/18h[b]	−76.15	−76.12	−76.29	24.88	30.87	16.50
17e/18e[c]	−74.92	−74.86	−74.75			
17f/18f[c]	−74.94	−74.87	−74.48			
17g/18g[c]	−75.06	−75.01	−74.61			
17h/18h[c]	−75.04	−74.99	−74.59			

[a] In $CDCl_3$. [b] $\delta(CF_3)$ of the $O{=}P(CO_2CH_2CF_3)_2$ group. [c] $\delta(CF_3)$ of the $CO_2CH_2CF_3$ group.

studies, the intramolecular hydrogen bondings C═O···H−O and P═O···H−O and C═O···H−N and P═O···H−N H-bonds should be very important in determining the configurations. A priori, the latter two N−H···O H-bonds are weaker than the O−H···O bonds. A previous observation was that the stronger the bond, the higher is the corresponding δ value (i.e., at a lower field). Another observation is that a bond to a certain ester group in **3** has a nearly constant δ(OH) regardless of the second activating ester group.[5,7b]

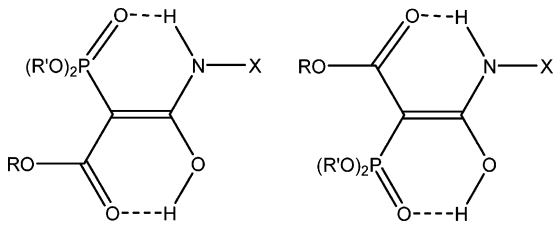

***E*-21**	R = Me, R' = Me	***Z*-21**
***E*-22**	R = CF_3CH_2 , R' = Me	***Z*-22**
***E*-23**	R = $(CF_3)_2CH$, R' =Me	***Z*-23**
***E*-24**	R = Me, R' = CF_3CH_2	***Z*-24**
***E*-25**	R=CF_3CH_2, R' = CF_3CH_2	***Z*-25**

The question for our systems concerns the relative strengths of P═O···H−O vs C═O···H−O bonds as a function of the substituent R. Qualitatively, the data suggest that the relative order changes when the number of fluorine atoms in the ester (series a) or in the phosphonate (series d) group changes. The presence of two hydrogen bonds in each enol complicates the issue. The easiest way to unequivocally evaluate the δ(OH) values of both the P═O···H−O and the P═O···H−N bonds in our system would be to obtain the values for compounds **13a-e** (series c) where both hydrogen bonds are present simultaneously.

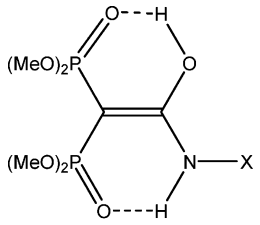

13

Since the $O{=}P(OMe)_2$ group is a better hydrogen bond acceptor than a CO_2Me group[18] (see below), we assumed that the doubly $O{=}P(OMe)_2$-activated systems **13** will show a higher K_{enol} than the doubly activated CO_2Me system **3**, $R^1 = R^2 =$ Me, which show ca. 7% enol in $CDCl_3$ when X = Ph.[4] However, the ^1H NMR spectra of all the five **12a−e/13a−e** systems in $CDCl_3$ at either 298 or 240 K displayed no signal ≥10 ppm. The possibility that the OH is lost in the baseline due to a coalescence process as found for ═C(CN)CO_2Me activated systems[8] is excluded since the signal should then be observed at the lower temperature, in contrast to the observation. Moreover, in the ^{13}C NMR C/H coupled spectra of all five systems, the C_β carbon at 47.4−48.4 ppm appears as a doublet of triplets due to coupling with both the geminal hydrogen ($^1J_{CH}$ = 135.1−135.5 Hz) and the geminal phosphorus ($^1J_{CP}$ = 127.5−129.1 Hz). No vinylic carbon was observed. Likewise, the ^{31}P NMR spectra displayed only one signal at 16.40−17.81 ppm. Consequently, all systems display exclusively the amide structures **12a−e** in solution. This is also the solid-state structure. X-ray diffraction of **12d**/**13d** showed the amide **12d**. Its CIF is in the Supporting Information.

We ascribe the absence of ≤2% (the limit of detection) of the enols **13** to the fact that the two geminal $O{=}P(OMe)_2$ groups create a too sterically congested situation for generating the enol in which both groups should preferably be in the same plane. This is reflected in the calculated structure of enol **13b** (Figure 3) which clearly show that the two $O{=}P(OMe)_2$ groups are above and below the ═C(OH)NHPh plane; i.e., the double bond is twisted and the conjugation necessary for the enol formation (eq 1) is reduced.

Based on the observation in systems ***E***- and ***Z*-3** that δ(OH) for a O−H···O═C-OR hydrogen bonding is nearly constant when R is constant,[5] but that it is reduced by ca. 1 ppm when R changes first for Me → CF_3CH_2 and then further by ca. 0.7 ppm for the change CF_3CH_2 → $(CF_3)_2CH$, we expect a similar change in δ(OH) for the **21** → **22** → **23** (or **24** → **25**) changes, provided that the $O{=}P(OR')_2$ group has a minor influence on this hydrogen bond. This was indeed found for the assigned *E*-enol, where the change R = Me → CF_3CH_2 → $(CF_3)_2CH$ [***E*-21** → ***E*-22** → ***E*-23**] result in corresponding average changes in δ(OH) of 1.02−0.83 ppm for *N*-Ar and of 0.92−0.76 ppm for *N*-Alk substituents (Table 5b). The changes of δ(OH) for

(18) Modro, A. M.; Modro, T. *Can. J. Chem.* **1999**, *77*, 890.

TABLE 5. δ(OH) and δ(NH) Differences

(a) Maximum Solvent Effect on the Values

compd	δ(OH,THF-d_8) − δ(OH,CCl_4)		δ(NH,THF-d_8) − δ(NH,CCl_4)	
	E	*Z*	*E*	*Z*
7	0.42−0.65	0.46−0.70	0.39−0.64	0.37−0.47
18	0.41−0.52	0.49−0.71	0.52−0.63	0.33−0.41

(b) Differences as a Function of the Ester Group

N-substituent		Δδ(OH,*E*-enol)		Δδ(OH,*Z*-enol)		Δδ(NH,*E*-enol)		Δδ(NH,*Z*-enol)	
		δ(**7a**−**e**) − δ(**7f**−**j**)	δ(**7f**−**j**) − δ(**7k**−**o**)	δ(**7a**−**e**) − δ(**7f**−**j**)	δ(**7f**−**j**) − δ(**7k**−**o**)	δ(**7a**−**e**) − δ(**7f**−**j**)	δ(**7f**−**j**) − δ(**7k**−**o**)	δ(**7a**−**e**) − δ(**7f**−**j**)	δ(**7f**−**j**) − δ(**7k**−**o**)
Ar	range	0.95−1.09	0.76−1.01	−0.17 to −0.27	−0.07 to −0.28	−0.16 to −0.27	−0.23 to −0.11	0.25−0.37	0.24−0.32
	avg (no. of pairs)	1.02 ± 0.04 (11)	0.83 ± 0.07 (10)	−0.21 ± 0.02 (7)	−0.16 ± 0.08 (8)	−0.21 ± 0.04 (10)	−0.16 ± 0.03 (12)	0.32 ± 0.04 (12)	0.28 ± 0.03 (12)
Alk	range	0.86−0.95	0.66−0.86	−0.16 to −0.25	−0.13 to −0.22	−0.16 to −0.24	−0.17 to −0.24	0.20−0.30	0.15−0.25
	avg (no. of pairs)	0.92 ± 0.02 (8)	0.76 ± 0.07 (8)	−0.20 ± 0.03 (8)	−0.19 ± 0.03 (8)	−0.21 ± 0.02 (8)	−0.20 ± 0.02 (8)	0.27 ± 0.02 (8)	0.22 ± 0.02 (8)

(c) Differences between *E*- and *Z*-Enols

N-substituent		Δδ(OH)(*E*-enol − Z-enol)					Δδ(NH)(*E*-enol − Z-enol)				
		7a−**e**	**7f**−**j**	**7k**−**o**	**18a**−**d**[a]	**18e**−**h**[a]	**7a**−**e**	**7f**−**j**	**7k**−**o**	**18a**−**d**[a]	**18e**−**h**[a]
Ar	range	1.51−1.78	0.27−0.60	−0.33 to −1.11	2.33−2.67	1.21−1.58	−0.09 to −0.44	0.14−0.54	0.52−1.02	−0.63 to −0.94	−0.14 to −0.46
	avg (no. of pairs)	1.63 ± 0.07 (9)	0.42 ± 0.10 (7)	−0.59 ± 0.30 (12)	2.53 ± 0.10 (13)	1.42 ± 0.08 (16)	−0.21 ±0.10 (11)	0.36 ± 0.11 (12)	0.79 ± 0.13 (12)	−0.77 ± 0.11 (16)	−0.29 ± 0.10 (16)
Alk	range	1.51−1.83	0.40−0.76	−0.20 to −0.58			−0.13 to −0.42	0.06−0.34	0.44−0.79		
	avg (no. of pairs)	1.68 ± 0.08 (8)	0.56 ± 0.09 (8)	−0.39 ± 0.12 (8)			−0.29 ± 0.07 (8)	0.19 ± 0.07 (8)	0.60 ± 0.08 (8)		

(d) Differences between Systems **7** and **18**

	Δδ(OH) (*Z*-enol)		Δδ(NH) (*E*-enol)	
	δ(**7a**−**e**)[b] − δ(**18a**−**d**)	δ(**7f**−**j**)[c] − δ(**18e**−**h**)	δ(**7a**−**e**)[b] − δ(**18a**−**d**)	δ(**7f**−**j**)[c] − δ(**18e**−**h**)
range	0.84−1.14	0.92−1.21	0.18−0.61	0.38−0.60
avg (no. of pairs)	0.98 ± 0.06 (13)	1.04 ± 0.06 (16)	0.47 ± 0.08 (16)	0.50 ± 0.06 (16)

[a] Including all four *N*-substituents [b] Excluding **7c**. [c] Excluding **7h**.

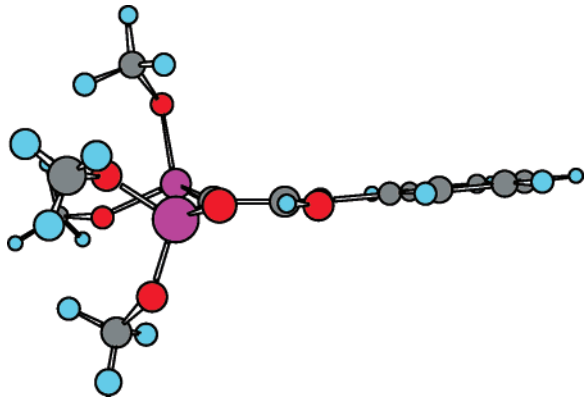

FIGURE 3. Sideview of the B3LYP/6-31G**-calculated structure of **13b** which shows the nonplanarity of the $[O{=}P(OMe)_2]_2C{=}C$ moiety.

system **4** for the Me → CF_3CH_2 → $(CF_3)_2CH$ changes are ca. 1.0 and 0.75 ppm, respectively.[7a,b] From this analogy in solution the *E*-enol is the one with O−H···O=C-OR hydrogen bond with the δ values assigned to it in Table 2. Further support arises from comparison of the analogous systems **7** and **18** (***E*-21** and ***E*-24** and ***E*-22** and ***E*-25**). For the *E*-enol the Δδ(OH) values are negligible, indicating that the OH is not bonded to the P=O group, since δ(OH) for **18** in which the P=O group is a weaker hydrogen bond acceptor than **7** should have been lower than for **7**. Moreover, these differences apply for both the **18a**−**d**/**7a**,**b**,**d**,**e** and the **18e**−**h**/**7f**,**g**,**i**,**j** pairs which are −0.12 ± 0.02 and −0.13 ± 0.02 ppm, respectively, supporting this conclusion for both O−H···O=C−OR (R = Me, CF_3CH_2) hydrogen bonds. This applies to all solvents studied, although the differences in CCl_4 are smaller (−0.06 ± 0.01 and −0.04 ± 0.01, respectively).

The δ(NH) for the *Z*-isomers should behave similarly since the NH is hydrogen bonded to the O=C−OR. They are 0.32 (0.27) and 0.28 (0.22) ppm for *N*-Ar(*N*-Alk) groups for the changes in R of Me → CF_3CH_2 → $(CF_3)_2CH$, ***Z*-21** → ***Z*-22** → ***Z*-23** (or ***Z*-24** → ***Z*-25**). The differences resemble the related changes in systems **3** and **4**.[5,7a,b]

By a similar argument, δ(OH) of the *Z*-enols and δ(NH) of the *E*-enols should also be nearly constant since in both there are identical O−H···O=$P(OMe)_2$ and N−H···O=$P(OMe)_2$ hydrogen bonds in series **7**, provided that the CO_2R group does not influence the δ(OH). However, both δ(OH,*Z*-enol) and δ(NH,*E*-enol) increase by ca. 0.20 ppm for each of the changes Me → CF_3CH_2 → $(CF_3)_2CH$ in R. This secondary effect which is still unclear, may arise from transmitting the EW effect of R group through C=C double bond.

The reduction of the δ(OH) values of the *Z*-enol by the CF_3 groups should be more pronounced on reducing the basicity of the hydrogen-bonded P=O, when the MeO groups of **7** are replaced by the CF_3CH_2O groups of **18**. Indeed, a significant average decrease of 0.98 and 1.04 ppm for the change when R of the CO_2R is Me or CF_3CH_2 was found. For the weaker N−H···O=P hydrogen bond of the *E*-enol the effect should be

significant but smaller, and values of 0.47 and 0.50 for Me and CF_3CH_2, half of those given above were found for δ(OH,*E*-enol) and δ(NH,*Z*-enol) were observed.

^{13}C, ^{19}F and ^{31}P NMR Data. (a) ^{13}C Data. Selected ^{13}C NMR chemical shifts are given in Table 3. The relevant signals are C_β and C_α of the *E*- and *Z*- enols and the amide, the CH_2 in the $(R'O)_2PO$ group and the ester carbonyl. The δ values are given only in $CDCl_3$ for several compounds, except for three systems for which the values are given in five solvents in order to demonstrate the solvent effect. The full data are provided in Table S2 of Supporting Information.

The amide is recognized by its CH signal which appears at the narrow range of 52.2−54.4 ppm in $CDCl_3$ (52.0−54.83 ppm in all solvents) and in the C/H coupled spectra as a doublet of doublets due to both C−H and C−P coupling ($^1J_{CH}$ = 127.9−133.4 Hz, $^1J_{CP}$ =120.8−136.6 Hz for **6/7** and $^1J_{CP}$ = 129.4−141.3 Hz for **17/18**). In contrast, the enol C_β which appears at 56.8−64.2 ppm, is easily distinguishable since it appears as a doublet, being coupled to the P with a $^1J_{CP}$ = 201−211.8 Hz for **6/7** and 212.1−222.1 Hz for **17/18**. The *N*-substituent effect on $\delta(C_\beta)$ is C_6F_5 > Ph > *p*-An > Alk. C_α of the enols appears as a doublet at δ 170.2−173.8 with $^2J_{CP}$ = 16.3−20.3 Hz. Consequently, $\Delta_{\alpha,\beta}$, which may be regarded as a crude measure of the polarity of the "C=C" bond of the enol (cf. structure **1b**) is >113 ppm, a value higher than that found for the corresponding diester systems.[5,7b,c] The amide N*C*=O signal is a doublet at δ 157.4−161.5 ppm with $^2J_{CP}$ = 4.5−6.4 Hz. Assignment of signals to the *E*- and *Z*-enols is based on their relative intensities and comparison with the intensities in the ^{1}H NMR spectra. Consistently, C_β, C_α, and *C*O_2R of the *E*-enol are at a lower field than for the *Z*-enol, and this feature can be used as diagnostic. For C_α the differences are 1.0 ± 0.2 for **7c**−**o** and 1.5 ± 0.3 for **18a**−**g**. For C_β the differences are 2.3 ± 0.3 for **7c**−**o** and 1.8 ± 0.1 for **18a**−**g** and for δ(*C*O_2R) they are larger, being 4.8 ± 0.1 ppm for **7c**−**o** and 5.13 ± 0.10 for **18a**−**g**. We ascribe these differences to the stronger O−H···O=C hydrogen bond to CO_2R in the *E*-enol than in the weaker N−H···O=C hydrogen bond in the *Z*-enol. This is supported by the opposite differences in the ^{31}P NMR (Table 4) where $\delta(^{31}P)$ is higher by 6 − 7.5 ppm for the *Z*-enol where the P=O is hydrogen bonded in the stronger O−H···O=P hydrogen bond than in the *E*-enol with the N−H···O=P bond. This is due to electron-withdrawal by the hydrogen bond from the M=O (M= C, P), which increases with its strength. The ester CO signals are at a lower field than the amide signals. The ***C***H_2OPO signals of **6** are at the same region as the amide CH, and the CH_2 of *C*F_3CH_2OPO of **17** is at lower field than the amide CH. In the uncoupled spectra these signals of the amide appear mostly as two doublets in **6** or as two quartets of doublets in **17** ($^2J_{CP}$ = ca. 6.7 Hz). The doubling of the signals is ascribed to the C_β chiral center and helps in unequivocally assigning these signals to the amide.

(b) ^{19}F NMR Data. Selected $\delta(^{19}F)$ NMR values in $CDCl_3$ using $CFCl_3$ as the reference are given in Table 4. The complete data are in Table S3 in the Supporting Information. In the noncoupled spectrum of the trifluoro derivatives **6f**−**j**/**7f**−**j** three singlets are observed in all solvents, except for DMSO-d_6. In DMSO-d_6, only one signal, for the amide, is observed, except for **6i**−**j**/**7i**−**j** where traces of the *Z*-enols were also observed. In the H−F coupled spectrum all signals are triplets ($^3J_{HF}$ = 7.2−10.9 Hz). The signals are identified by comparison with the relative integrations in the ^{1}H NMR data. The order of the negative δ(F) values is amide (less negative) > *Z*-enol > *E*-enol. The differences between the two enols are small, between 0.02 and 0.07 ppm.

For the hexafluoro derivatives **6k**−**o**/**7k**−**o** only two signals are observed in all solvents except DMSO-d_6 due to overlap of the *E*-enol and *Z*-enol signals. The δ(F) values for the amides are less negative. In the H−F coupled spectrum all signals are split to doublets ($^3J_{HF}$ = 4.9 − 7.2 Hz) by the methine hydrogen. For **6l/7l** two amide signals are observed in the non-coupled spectra in DMSO-d_6 (see above), which appear as multiplets in the coupled spectrum. As in the ^{1}H NMR spectrum, **6n**−**o**/**7n**−**o** display the *Z*-enol signals in DMSO-d_6, as well as traces of ***Z*-7k** and ***Z*-7l**.

The δ(F) values are less negative for the hexa-F than for the tri-F of the three species.

For systems **17a**−**d**/**18a**−**d** there is only one type of fluorine signal in the $(CF_3CH_2O)_2P$=O group. For **17e**−**h**/**18e**−**h** there are two types of fluorine signals, for $(CF_3CH_2O)_2P$=O and CF_3-CH_2OCO. The values for the former group in **17a**−**h**/**18a**−**h** are more negative than those for the latter ones in **6f**−**j**/**7f**−**j**.

(c) ^{31}P NMR Data. Selected ^{31}P NMR data in CCl_4 only are given in Table 4 based on H_3PO_4 as a reference. The complete data are in Table S3 in the Supporting Information. ^{31}P NMR is a better quantitative probe than ^{19}F NMR since the signals are much better separated. Indeed, the relative integration of the ^{31}P signals is closer in most cases to those of the ^{19}F spectra than to those of the ^{1}H NMR spectra (Table S4). The three signals observed in most cases were identified by their integration and splitting pattern in the H−P coupled spectrum. In the **6**/**7** series the δ(P) signal of the *Z*-enol appears at the lowest field of 29.17 − 34.78 ppm in $CDCl_3$ (28.92 − 35.04 ppm in all solvents), followed by the *E*-enol signal at 20.38 − 27.73 ppm as an heptet for **6/7** or quintet for **17/18**, due to coupling with the two MeO groups. For the amide δ(P) is at a higher field of 12.62−18.67 ppm. The α-H-coupled signals display a nine-line multiplet for **6/7** and eight-line multiplet for **17/18** due to overlap of few lines. The difference in ppm $\Delta\delta = \delta$(*Z*-enol) − δ(*E*-enol) is appreciable, and slightly increase with the increase in the number of fluorine atoms in the ester group. For **7a**−**e** it is 7.15 ± 0.19, for **7f**−**j** it is 7.32 ± 0.12 and for **7k**/**7o** it is 7.59 ± 0.19. In the $(CF_3CH_2O)_2P$=O-substituted systems **18**, the differences are smaller and within the combined experimental errors: 5.92 ± 0.04 for **18a/18d** and 5.99 ± 0.03 for **18e/18h**.

The Cyano-Activated Systems. The four cyano-activated systems **9a**−**d**/**10a**−**d** were analyzed by ^{1}H NMR spectra. At 298 K in $CDCl_3$ the lowest field signals were for the amides: at 8.83−9.12 ppm when X = Ar (**9a**−**c**) and at 6.53 ppm for X = *t*-Bu (**9d**). The amides were the major species as judged from their CH signals. In addition, small signals at 7.58−7.98 ppm **(10a**−**c)** and 5.58 ppm (**10d**) with 0.9−7.1% intensities of the amide signals were observed. On cooling to 240 K, these signals shifted to 8.09−8.66 and 5.66 ppm, and small new signals (except for **9c**) with identical intensity appeared at ca. 13.4 ppm. In analogy with other systems we ascribe the new low field signal to an enolic OH, and the higher field signal to the NH of the enol. The assignment is corroborated by the ^{31}P NMR spectra which display one small broad signal for X = Ph, *p*-An and an heptet ($^3J_{PH}$ = 11.57 Hz) for X = C_6F_5 at a low field of 27.58−28.97 ppm, with intensities of 3.7−7.3% of the intensity of the main amide species **9a**−**c** at 12.84−13.64 ppm (d of heptets, $^2J_{HP}$ = 24.25−24.96 Hz, $^3J_{HP}$ = 11.44−11.68 Hz). The ^{1}H and

^{31}P NMR spectra enable calculation of K_{enol} values at 298 K of 0.01−0.08 in $CDCl_3$.

The *t*-Bu derivative **9d**/**10d** already shows at 298 K in $CDCl_3$ or in 2:1 CCl_4/$CDCl_3$ a broad signal at 13.22 ppm with 6.5% intensity of the amide signal at 6.53 ppm, as well as a signal of the same intensity at 5.58 ppm. On lowering the temperature the low field signal sharpens. Both signals were ascribed to the enol **10d**. In the ^{31}P NMR spectrum a signal at 29.97 ppm (hept, $^3J_{PH}$ = 11.66 Hz) with 6.6% of the intensity of the amide signal at 14.19 ppm (d of hept, $^2J_{PH}$ = 24.57 Hz, $^3J_{PH}$ = 11.65 Hz) was observed.

The less sensitive ^{13}C NMR spectra in $CDCl_3$ had shown signals consisting only with the amide **9** structures. The CH carbons at 38.5−39.2 ppm were doublets of doublets due to coupling with both the geminal hydrogen and phosphorus ($^1J_{CH}$ = 135.1−135.5 Hz, $^1J_{CP}$ = 127.9−129.1 Hz).

The behavior of the cyano-activated systems resembles that of some (CN)CO_2R activated systems ***Z*-4** with *N*-Ar = Ph or *p*-BrC_6H_4, in the absence of an enolic OH signal at rt and its appearance on cooling.[7a] The reason for this may be an exchange (and coalescence of signals) of the amide and the enol at rt. However, these systems are fully enolic both in the solid state and in solution. Apparently, the activation by a single $(MeO)_2P$═O group is lower than that of a CO_2Me group when both appear together with a CN group.

K_{enol} and *E*/*Z* Values. Solvent and Substituent Effects. The enols/amide distributions and the derived K_{enol} values and *E*/*Z* ratios are given in Table 6 for all of the systems, except **12**/**13** in all of the solvents studied. The ratios were determined by integration of the NH signals, and occasionally of the amide CH signals in the ^{1}H NMR spectra, by integration of the three ^{31}P signals, and when available of the three ^{19}F NMR signals. There is a close similarity (within 1%) in the product distributions derived from the ^{1}H and ^{31}P spectra, which is somewhat better than with the ^{19}F derived values since the ^{19}F signals are less spread. The enols/amide ratios are averages of the two first values, or of the three (in parentheses) values. The integrations for all compounds are given in Table S4 in the Supporting Information.

The three signals are observed for all systems, except for the bisphosphonates **12**/**13** where only the amides **12** were observed. They were observed in all solvents except for DMSO-d_6 in which mostly, but not always, only the amide signal was observed.

The solvent effect for 17 out of the 23 systems for which data are available in five solvents follow the order for K_{enol} of CCl_4 > $CDCl_3$ > THF-d_8 > CD_3CN > DMSO-d_6. This order differs from the order of δ(OH) or δ(NH) at 298 K which is THF-d_8 > CD_3CN > $CDCl_3$ > CCl_4 (Table 2).

Changing the substituent in the ester group of systems **6**/**7** causes a significant change in K_{enol}. The amide is the major species for the CO_2Me esters in all solvents, the enols predominate in the less polar solvents for the $CO_2CH_2CF_3$ esters, and the enols are the major species in all solvents , except DMSO-d_6 for the $CO_2CH(CF_3)_2$ esters. Roughly, K_{enol} increases by an order of magnitude when R in the ester changes from Me to CF_3CH_2, and by a factor of 7 when R changes from CF_3CH_2 to $(CF_3)_2CH$. The changes in log K_{enol} are roughly the same but in the opposite direction, as those in δ(OH, ppm) for changes in these R's. Obviously, when the K_{enol} is very high (>100), the numbers and their ratios are very approximate, since a fraction of a percent change in one component changes K_{enol} enormously.

The increase in K_{enol} on changing the substituent from R = Me to CF_3CH_2 in the ester group for systems **17**/**18** with the $(CF_3CH_2O)_2P$═O groups is also appreciable: by 8.5−15-fold in $CDCl_3$ and by 4.9−6.1-fold in CCl_4, THF-d_8, and CD_3CN. The change caused by introducing six fluorine atoms in the phosphonate group is shown by comparing K_{enol} values for corresponding compounds in series **6**/**7** and **17**/**18**. K_{enol} (**17**/**18**) > K_{enol} (**6**/**7**) when R is Me (CF_3CH_2) by average values of 9.0 (4.3) in CCl_4, 10.3 (10) in $CDCl_3$, 2.5 (1.7) in THF-d_8 and 5.0 (3.1) in CD_3CN. The increase in K_{enol} on increasing the number of fluorine atoms in the carboxylic ester or the phosphonate ester fit the expectation of higher % enol with higher electron-withdrawal by the activating Y,Y′ groups. The effect is smaller in the phosphonate ester (despite the six fluorine atoms) than by a carboxylic ester. Tentatively, the steric hindrance of the former group offsets the EWG effect. The small effect in THF-d_8 may be connected with its hydrogen bonding ability.

The very low K_{enol} values of the CN phosphonate systems in $CDCl_3$ apparently contrast the higher activation of a $(MeO)_2P$═O than of a CO_2Me group in other systems. The larger steric effect for $(MeO)_2P$═O suggested above for the absence of enols **13** in solution, although $(MeO_2C)_2C$═C(OH)-NHPh is observable in $CDCl_3$,[4] may partially account for the effect.

The *N*-aryl substituent effect for compounds ***Z*-4** gives a Hammett log K_{enol} vs σ correlation with a small negative slope, i.e., electron-donating substituents increase K_{enol}.[7a] For compounds **6**/**7** the effect is not large and less systematic. The changes from **6**−**7f** to **6**−**7h** and from **6**−**7k** to **6**−**7m** parallel those for compounds **4**, but for **6**−**7a** to **6**−**7c** K_{enol} first decrease and then increase again. For pairs of *N*-*p*-An and *N*-Ph in **17**/**18** K_{enol} is higher for the more electron donating *p*-An.

For *N*-alkyl substituents K_{enol}(*i*-Pr) > K_{enol}(*t*-Bu), and K_{enol}-(*i*-Pr) is mostly the highest among all the *N*-substituted systems, as found for systems **3** where for K_{enol} *i*-Pr > *p*-An > Ph.[5]

The *Z*-enol predominates in all the ***E*-7**/***Z*-7** systems; i.e., *E*/*Z* ratios are <1. They decrease when R in CO_2R carries more fluorine atoms, e.g., in $CDCl_3$ *E*/*Z* = 0.75 (*N*-Ph) and 0.58 (*N*-*i*-Pr) when R= Me, 0.33 (*N*-Ph) and (0.30) (*N*-*i*-Pr) for R = CF_3CH_2 and 0.16 (*N*-Ph), and 0.13 (*N*-*i*-Pr) when R = $(CF_3)_2$-CH. In each case the ratios are higher in the chlorinated than in the more polar solvents. In contrast, for ***E*-18**/***Z*-18**, R = CO_2-Me the *E*/*Z* ratio >1, but for R = CF_3CH_2 it is <1. The other characteristic features are the same as for the ***E*-7**/***Z*-7** systems.

There is a delicate balance between several effects to determine the stability difference between the *E*- and *Z*-enols. The *E*/*Z* ratio in series **7** is <1. When the $(MeO)_2P$═O groups in **7** are replaced by the more EW $(CF_3CH_2O)_2P$═O groups in **18** the O−H···O═P hydrogen bond in ***Z*-18** become weaker and the effect is more pronounced than on the N−H···O═P bond in ***E*-18**. Consequently, the *E*/*Z* ratio increases and becomes >1. For **18e**−**h** the same effect also increase the *E*/*Z* ratio over that for **7a**−**e**, but since R = CF_3CH_2, the *E*/*Z* value for **7f**−**j** is already lower than for **7a**−**e**, and the increased *E*/*Z* value for **18e**−**h** remains <1.

Relationship between the Stability of the *E*/*Z* Isomers and the Chemical Shifts. In compounds **3** and **4** the order of δ-(OH) and δ(NH) values as a function of R was the same as the order of stability of the species and correlations were observed between δ(OH) and δ(NH) and K_{enol} values.[5] The higher the δ(OH), the higher the K_{enol} value. This is not the case in the present systems. The $\Delta\delta$(OH)(*E*-enol − *Z*-enol) values change from high positive values of 1.68 (*N*-Ar and *N*-Alk) for **7a**−**e** to 0.42 (*N*-Ar) and 0.56 (*N*-Alk) for **7f**−**j** to negative values of −0.68 (*N*-Ar) and −0.39 (*N*-Alk) for **7k**−**o**. Consequently, there is an approximate additivity of ca. 1 ppm for addition of 3 and

TABLE 6. Percentage of *E*-Enol, *Z*-Enol, and Amide, K_{enol}, and *E*/*Z*-Enol Ratio for the Amide/Enols at 298 K in Different Solvents[a]

compd	solvent	*E*-Enol	*Z*-Enol	amide	K_{enol}	*E*/*Z*
6a/7a	CCl_4	20.7	27.8	51.5	0.94	0.74
	$CDCl_3$	4.35	5.85	89.8	0.11	0.74
	THF-d_8	4.0	7.5	88.5	0.13	0.53
	CD_3CN	0.6	1.2	98.2	0.018	0.50
	DMSO-d_6			100	≤0.01	
6b/7b	CCl_4	13.8	23.9	62.3	0.61	0.58
	$CDCl_3$	3.8	5.1	91.1	0.098	0.75
	THF-d_8	2.95	5.05	92.0	0.087	0.58
	CD_3CN	0.45	0.90	98.65	0.014	0.50
	DMSO-d_6			100	≤0.01	
6c/7c	CCl_4	17.3	25.9	56.8	0.76	0.66
	$CDCl_3$	4.20	5.75	90.05	0.11	0.73
	THF-d_8	1.35	4.35	94.30	0.06	0.31
	CD_3CN	0.35	1.05	98.60	0.014	0.33
	DMSO-d_6			100	≤0.01	
6d/7d	CCl_4	18.4	34.1	47.5	1.11	0.54
	$CDCl_3$	5.0	8.6	86.4	0.16	0.58
	THF-d_8	8.8	20.2	71.0	0.41	0.44
	CD_3CN	1.2	2.7	96.1	0.041	0.44
	DMSO-d_6			100	≤0.01	
6e/7e	CCl_4	15.0	24.9	60.1	0.66	0.60
	$CDCl_3$	3.45	6.0	90.55	0.10	0.58
	THF-d_8	5.3	12.2	82.5	0.21	0.43
	CD_3CN	0.8	1.55	97.65	0.024	0.52
	DMSO-d_6			100	≤0.01	
6f/7f	CCl_4	19.6 (21.3)	70.4 (68.5)	10.0 (10.2)	9.0 (8.8)	0.28 (0.31)
	$CDCl_3$	13.35 (14.5)	42.4 (41.5)	44.25 (44)	1.26 (1.27)	0.32 (0.35)
	THF-d_8	8.6 (8.7)	37.9 (37.2)	53.5 (54.1)	0.87 (0.85)	0.23 (0.23)
	CD_3CN	2.25 (2.5)	10.55 (10.6)	87.2 (86.9)	0.15 (0.15)	0.21 (0.24)
	DMSO-d_6			100	≤0.02	
6g/7g	CCl_4	19.7 (20.4)	67.5 (66.6)	12.8 (13.0)	6.8 (6.7)	0.29 (0.31)
	$CDCl_3$	12.7 (14.1)	38.9 (38.1)	48.4 (47.8)	1.07 (1.09)	0.33 (0.37)
	THF-d_8	6.25 (7.1)	28.8 (28.6)	64.95 (64.3)	0.54 (0.56)	0.22 (0.25)
	CD_3CN	1.9 (1.9)	8.2 (8.3)	89.9 (89.8)	0.11 (0.11)	0.23 (0.23)
	DMSO-d_6			100	≤0.02	
6h/7h	CCl_4	17.2	67.5	15.3 (15.3)	5.53 (5.53)	0.25
	$CDCl_3$	11.0 (11.4)	37.1 (36.4)	51.9 (52.2)	0.93 (0.92)	0.30 (0.31)
	THF-d_8	3.9 (3.8)	28.0 (28.7)	68.1 (67.5)	0.47 (0.48)	0.14 (0.13)
	CD_3CN	1.2	8.0	90.8 (90.5)	0.10 (0.10)	0.15
	DMSO-d_6			100	≤0.02	
6i/7i	CCl_4	19.6 (20.4)	71.9 (71.2)	8.5 (8.2)	10.8 (11.2)	0.27 (0.29)
	$CDCl_3$[b]	14.85 (15.2)	48.7 (48.9)	36.45 (35.9)	1.74 (1.79)	0.30 (0.31)
	THF-d_8	11.0 (11.5)	60.0 (60.5)	29 (28)	2.45 (2.57)	0.18 (0.19)
	CD_3CN	4.8 (4.7)	22.9 (23.1)	72.3 (72.2)	0.38 (0.39)	0.21 (0.21)
	DMSO-d_6		4.2 (4.2)	95.8 (95.8)	0.04	
6j/7j	CCl_4	18.0 (18.7)	70.4 (69.7)	11.6 (11.6)	7.62 (7.62)	0.26 (0.27)
	$CDCl_3$[b]	12.8 (13.2)	42.0 (42.2)	45.2 (44.6)	1.21 (1.24)	0.30 (0.31)
	THF-d_8	9.6 (10.3)	50.1 (50.2)	40.3 (39.5)	1.48 (1.53)	0.19 (0.21)
	CD_3CN	3.1 (3.2)	14.5 (14.4)	82.4 (82.4)	0.21 (0.21)	0.21 (0.22)
	DMSO-d_6		2.7 (2.7)	97.3 (97.3)	0.028 (0.028)	
6k/7k	CCl_4	11.6	86.8	1.6 (1.7)	61.5 (57.8)	0.13
	$CDCl_3$	13.1	80.6	6.3 (6)	14.9 (15.7)	0.16
	THF-d_8	7.6	80.8	11.6 (11.9)	7.6 (7.4)	0.094
	CD_3CN	4.9	55.2	39.9 (40.4)	1.51 (1.48)	0.089
	DMSO-d_6		4.1	95.9 (95.4)	0.043 (0.048)	
6l/7l	CCl_4	11.9	86.2	1.9 (2)	51.6 (49)	0.14
	$CDCl_3$	12.9	79.9	7.2 (7.1)	12.9 (13.1)	0.16
	THF-d_8	7.0	74.6	18.4 (18.8)	4.43 (4.32)	0.094
	CD_3CN	4.5	47.9	47.6 (47.2)	1.10 (1.12)	0.094
	DMSO-d_6		2.7	97.3 (97.5)	0.025 (0.026)	
6m/7m	CCl_4	9.6	87.3	3.1 (3.6)	31.3 (26.8)	0.11
	$CDCl_3$	11.7	77.8	10.5 (10.3)	8.52 (8.71)	0.15
	THF-d_8	4.6	70.9	24.5 (24.7)	3.08 (3.05)	0.065
	CD_3CN	1.8	38.7	59.5 (58.7)	0.68 (0.70)	0.047
	DMSO-d_6		3.1[c]	96.9[c]	(0.032)[c]	
6n/7n	CCl_4	10.3	89.5	0.2	ca. 496	0.11
	$CDCl_3$	11.25	85.55	3.2 (3.23)	30.25 (29.93)	0.13
	THF-d_8	6.9	90.35	3.25 (3.17)	29.92 (30.55)	0.08
	CD_3CN	6.1	76.6	17.3 (16.8)	4.78 (4.95)	0.08
	DMSO-d_6		25.0	75.0 (75.1)	0.33 (0.33)	
6o/7o	CCl_4	10.0	89.6	0.4	249	0.11
	$CDCl_3$	11.6	83.1	5.1 (5.2)	17.9 (18.2)	0.14
	THF-d_8	7.15	85.9	6.95 (6.67)	13.4 (14.0)	0.08
	CD_3CN	5.6	65.2	29.2 (28.7)	2.42 (2.48)	0.09
	DMSO-d_6		15.4 (15.6)	84.6(84.4)	0.18 (0.18)	

Table 6 (Continued)

compd	solvent	*E*-enol	*Z*-enol	amide	K_{enol}	*E*/*Z*
9a/10a	$CDCl_3$		7.2	92.8	0.08	
			2.3[d]	97.7[d]	0.02[d]	
9b/10b	$CDCl_3$		4.0	96.0	0.04	
			1[d]	99[d]	0.01[d]	
9c/10c	$CDCl_3$		0.9[e]	99.1[e]	≤0.01[e]	
			4[c]	96[c]	0.04[e]	
			1.4[d]	98.6[d]	0.01[d]	
9d/10d	$CDCl_3$		6.6	93.4	0.07	
			5[d]	95[d]	0.05[d]	
17a/18a	CCl_4	55.0	31.8	13.2 (13.1)	6.58 (6.63)	1.72
	$CDCl_3$	31.1 (29.5)	20.1 (21.6)	48.8 (48.9)	1.05 (1.04)	1.55 (1.37)
	THF-d_8	14.0	11.2	74.8 (75.0)	0.34 (0.33)	1.25
	CD_3CN	4.5 (4.8)	3.7 (3.7)	91.8 (91.5)	0.09 (0.09)	1.22 (1.30)
	DMSO-d_6			100	≤0.02	
17b/18b	CCl_4	55.1	28.9	16.0 (16.0)	5.25 (5.25)	1.91
	$CDCl_3$	30.1 (31.4)	18.1 (16.2)	51.8 (52.4)	0.93 (0.91)	1.66 (1.94)
	THF-d_8	10.7	7.8	81.5 (81.4)	0.23 (0.23)	1.37
	CD_3CN	4.1	2.7	93.2 (92.7)	0.07 (0.08)	1.52
	DMSO-d_6			100	≤0.02	
17c/18c	CCl_4	56.5 (55.7)	35.0 (35.7)	8.5 (8.6)	10.7 (10.6)	1.61 (1.51)
	$CDCl_3$	36.7 (38.8)	27.1 (25.1)	36.2 (36.1)	1.76 (1.77)	1.35 (1.55)
	THF-d_8	23.1	22.2	54.7 (54.2)	0.83 (0.85)	1.04
	CD_3CN	9.5	7.8	82.7 (82.0)	0.21 (0.22)	1.22
	DMSO-d_6			100	≤0.02	
17d/18d	CCl_4	51.5 (52.1)	31.3 (30.8)	17.2 (17.0)	4.80 (4.88)	1.65 (1.69)
	$CDCl_3$	30.2 (30.0)	22.2 (21.8)	47.6 (48.2)	1.10 (1.07)	1.36 (1.38)
	THF-d_8	19.2	16.5	64.3 (64.7)	0.55 (0.55)	1.16
	CD_3CN	5.9	4.7	89.4 (89.0)	0.11 (0.12)	1.26
	DMSO-d_6			100	≤0.02	
17e/18e	CCl_4	41.4	56.4	2.2	44.5	0.73
	$CDCl_3$	40.6	53.4	6.0	15.7	0.76
	THF-d_8	21.3	38.9	39.8	1.51	0.55
	CD_3CN	11.6	21.0	67.4	0.48	0.55
	DMSO-d_6			100	≤0.02	
17f/18f	CCl_4	42.7	54.3	3.0	32.3	0.79
	$CDCl_3$	40.7	51.3	8.0	11.5	0.79
	THF-d_8	17.7	30.2	52.1	0.92	0.59
	CD_3CN	9.7	16.0	74.3	0.35	0.61
	DMSO-d_6			100	≤0.02	
17g/18g	CCl_4	40.1	59.7	0.2	499	0.67
	$CDCl_3$	38.0	56.9	5.1	18.6	0.67
	THF-d_8[b]	27.0	55.5	17.5	4.71	0.49
	CD_3CN	17.3	35.3	47.4	1.11	0.49
	DMSO-d_6		6.1	93.9	0.06	
17h/18h	CCl_4	40.2	55.7	4.1	23.4	0.72
	$CDCl_3$	36.6	53.7	9.7	9.31	0.68
	THF-d_8	23.9	44.3	31.8	2.14	0.54
	CD_3CN	14.1	25.1	60.8	0.64	0.56
	DMSO-d_6			100	≤0.02	

[a] Data for system **12/13**, which forms the amide exclusively are not given. The ratios are averages of integrations of the ^{1}H (NH) signals and ^{31}P signals (without parentheses) and of the ^{1}H, ^{31}P, and ^{19}F values (in parentheses) for the fluoro-containing compounds. [b] Based on OH and NH of amide due to a partial overlap of the NH signals of *E*- and *Z*-enols. [c] Based on ^{31}P NMR. No enol was observed by ^{1}H NMR. [d] Measured at 240K. [e] Based on ^{1}H NMR.

6 fluorine atoms in the ester group. Likewise, the sign of Δδ-(NH)(*E*-enol − *Z*-enol) also changed from −0.29 (*N*-Ar) and −0.36 (*N*-Alk) for **7a**−**c** to 0.36 (*N*-Ar) and 0.19 (*N*-Alk) for **7f**−**j** to 0.71 (*N*-Ar) and 0.58 (*N*-Alk) for **7k**−**o**. There is less than an additive change in Δδ(NH) of *ca*. 0.6 and 0.37 ppm for the 0F → 3F → 6F change.

From Table 6 the *Z*-enol is always formed in excess, except for **17a**−**d**/**18a**−**d** and hence, it is the more stable enol. This preferred stability increases with the increased number of fluorine atoms in the CO_2R.

Both facts fit a single pattern. The shift in Δδ(OH) with the number of fluorines in R of ***E*-7** is due to the decreasing hydrogen bond accepting ability by the C═O oxygen resulting since R is better EWG. The effect on the *Z*-enol should be smaller since the same P═O group is hydrogen bonded to the O−H in all systems. In practice δ(OH) is slightly increasing, probably the O−H bond is more acidic due to the increased electron-withdrawal from this bond by the remote ROC═O group. The weaker hydrogen bond to O−H in the *E*-isomer reduces its stability together with the slightly increased hydrogen bond strength of the *Z*-isomer which increases its stability, results in the parallel decrease of the *E*/*Z* ratios.

A complete analysis of the relative stabilities should take into account the other weaker hydrogen bonds to the N−H present in each enol. The decreased strength of the O−H···O═M (M = P, C) hydrogen bonds is accompanied by an increased strength of the N−H···O═M (M = C, P) hydrogen bond, so that the overall stability of the species reflects the energy difference between the two hydrogen bonds. This is the reason why the *E*/*Z* ratios, translated to energy differences of 0.17−1.8 kcal/mol for **6/7** and **17e**−**h**/**18e**−**h** and −0.3 to −0.13 kcal/mol for **17a**−**d**/**18a**−**d** are not large, enabling to see both ***E*-7** and ***Z*-7** (and ***E*-18** and ***Z*-18)** in solution. When one hydrogen bond cannot be formed, as in the cyano esters, due to the linear geometry of the CN group, only the *Z*-isomer is observed in solution.

The similarity between the enols of diesters with 0, 3, and 6 F atoms and the dialkoxyphosphinyl esters with a similar pattern of fluorine substitution is shown in a plot of the literature δ-

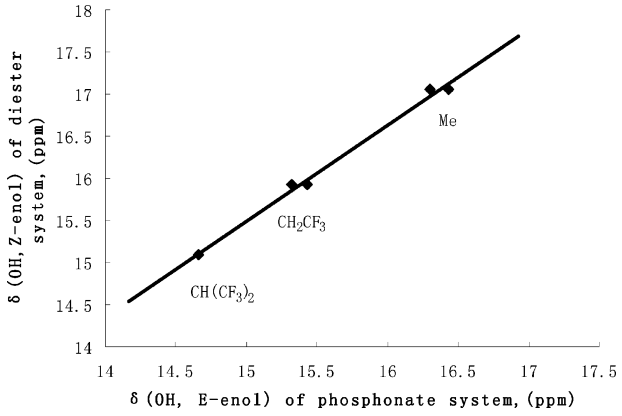

FIGURE 4. Plot of δ(OH, *Z*-enol) of the diesters **3** (*N*-substituents = Ph, *p*-An, *p*-MeC_6H_4, and *p*-BrC_6H_4[5] vs δ(OH, *E*-enol) of the dialkoxyphosphinyl ester systems **7** and **18** (*N*-substituents = Ph, *p*-An, and C_6F_5) in $CDCl_3$ at 298 K. δ(OH, *Z*-enol) = 1.14δ(OH, *E*-enol) − 1.161 (R^2 = 0.9933).

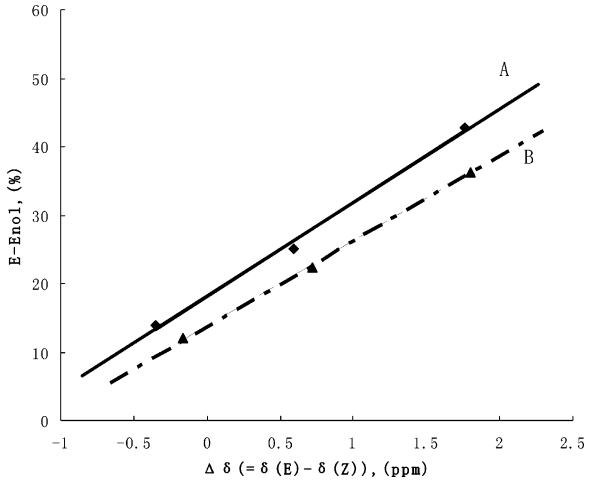

FIGURE 5. Plot of the average % *E*-enol in the enols mixture for **7a**−**e**,**f**−**j**,**k**−**o** vs the average $\Delta\delta$(OH) = δ(*E*-enol) − δ(*Z*-enol) in $CDCl_3$ at 298 K: (A) *N*-Ar groups, %*E*-enol = 13.71$\Delta\delta$ + 18.13 (R^2 = 0.9947); (B) *N*-alkyl groups, %*E*-enol = 12.47$\Delta\delta$ + 13.73 (R^2 = 0.9995).

(OH, *Z*-enol) of the diesters series vs the δ(OH, *E*-enol) in the phosphonate series (Figure 4). In both cases, the OH is hydrogen bonded to a CO_2R group, while the other group (Me ester or P ester) is constant. The excellent linearity (R^2 = 0.9933) and the slope of 1.14 indicate a similar behavior of the diesters and of the phosphonate esters.

A similar argument as for $\Delta\delta$(OH) applies also for the $\Delta\delta$(NH)(*E*-enol − *Z*-enol) except that due to the weaker N−H···O=M (M = P, C) bonds the effects are smaller.

Although the lower field signal is not always that for the more stable enol, we may expect a correlation between the abundance of one enol in the enols mixture and $\Delta\delta$(OH) between the two isomers, since both parameters are affected by the number of fluorine atoms in the ester group R. Indeed, a plot of the average percentage of the *E*-enol (100% [*E*-enol]/([*E*-enol] + [*Z*-enol]) vs $\Delta\delta$(OH) = δ(*E*-enol) - δ(*Z*-enol) in $CDCl_3$ at 298 K is linear, but depends on the *N*-substituent X. Figure 5 shows two parallel lines, one for the aryl (Ar = *p*-An, Ph) substituents and one for the alkyl (Alk = *i*-Pr, *t*-Bu) substituents, with slopes of 13.7 (R^2 = 0.9947) and 12.47 (R^2 = 0.9995). The inversion in the positions of δ(*E*-enol) and δ-(*Z*-enol) is reflected by the negative $\Delta\delta$(OH) value when R = $(CF_3)_2CH$.

Comparison of $(R'O)_2P$=O and CO_2R Groups. The difference in electron-withdrawing power of phosphonate and ester groups and of hydrogen bonding abilities of the phosphoryl and carbonyl groups affects the δ(OH), δ(NH), *E*/*Z* enol ratios and K_{enol} values, and their differences from those of compounds **3** and **4**. Evaluation of these differences is therefore necessary for understanding the behavior of our systems.

A single phosphonate ester is a better electron-withdrawing and somewhat better negative charge delocalizing substituent than a single methyl ester as judged by various types of Taft's, Hammett's, and Brown's σ parameters. For $(MeO)_2PO$ σ_R, σ_R^-, σ_m, σ_p^-, σ_p, and σ_p^+ are 0.21, 0.33, 0.46, 0.87, 0.59, and 0.73, respectively, and for CO_2Me they are 0.11, 0.30, 0.36, 0.74, 0.44, and 0.49, respectively.[19a] The σ* values are 2.45 ($(MeO)_2PO$)[19b] and 2.00 (CO_2Me).[19c]

The P=O group is a well-known strong hydrogen bond acceptor,[20] e.g., in an intramolecular hydrogen bond with OH in $HO(CH_2)_nP(=O)Ph_2$[20c] or in $(RO)_2P(=O)CH_2CH(OH)R'$,[21] but only a few works address the question of the relative hydrogen bond accepting ability in competition of a P=O with a C=O group. Deshielding of the P in 2-hydroxyalkylphosphonates was ascribed to a decreased π-donation from intramolecular hydrogen bonding between the P=O oxygen and the OH group.[21a] P=O···H−O bonding was also found in polymers and it is assumed that in the hydrogen bond the P=O becomes softer.[21b] By conformation analysis based on ^{1}H NMR spectra the "P=O" is favored over C=O in an intramolecular interaction with a β-OH group.[22] From pK_a's of P=O and C=O groups it was deduced that protonation of the former in ArCOPO(OH)-OPh is preferred over that of latter.[23]

Quantitative data on hydrogen bond parameters of the $(MeO)_2P$=O and CO_2Me groups for use in LFERs indicate that the former is a better hydrogen bond acceptor.[24] The only quantitative data relevant to our system comes from the IR $\Delta\nu$ shift measurements of the formation constants of the hydrogen bond adducts between phenol and RCH_2R' (R = R′ = MeCO, MeO_2C, $(EtO)_2P$=O) which give data on intermolecular competition, and for R = $(EtO)_2PO$, R′ = CO_2Et for intramolecular

(19) (a) Charton, M. In *The Chemistry of Cyclobutanes*; Rappoport, Z., Liebman, J. F., Eds.; Wiley: New York, 2005; Chapter 10, p 441. (b) Katzhendler, J.; Ringel, I.; Karaman, R.; Zaher, H.; Breuer, E. *J. Chem. Soc., Perkin Trans. 2* **1997**, 341. (c) Taft, R. W., Jr. In *Steric Effects in Organic Chemistry*; Newman, M. S., Ed.; Wiley: New York, 1956; Chapter 13, p 619.

(20) (a) Corbridge, D. C. E. *Phosphorus. An Outline of its Chemistry, Biochemistry and Technology*, 4th ed.; Elsevier: Amsterdam, 1990; Chapter 14.1. (b) Gramstad, T. *Spectrochim. Acta* **1963**, *19*, 1363. (c) Asknes, G.; Albriktsen, P. *Acta Chem. Scand.* **1966**, *22*, 1866. (d) Gramstad, T.; Storesund, H. J. *Spectrochim. Acta Part A* **1970**, *26A*, 426. (e) Bel'skii, V. E.; Bakeeva, R. F.; Kudryavtseva, L. A.; Kurguzova, M. A.; Ivanov, B. E. *Zh. Obshch. Khim. (Eng. Transl.)* **1975**, *43*, 2568. (f) Raevskii, O. A.; Gilyazov, M. M.; Levin, Y. A., *Zh. Obshch. Khim.* **1978**, *48*, 1053. (g) Bel'skii, V. E.; Ashrafullina, L. Kh. *Zh. Obshch. Khim. (Engl. Transl.*) **1979**, *49*, 1968.

(21) (a) Genov, D. G.; Tebby, J. C. *J. Org. Chem.* **1996**, *61*, 2454. (b) Alexandratos, M.; Zhu, X. *Macromolecules* **2005**, *38*, 5981.

(22) (a) Belciug, M. P.; Modro, A. M.; Modro, T. A. *J. Phys. Org. Chem.* **1992**, *5*, 787. (b) Belciug, M. P.; Modro, P. A.; Wessels, P. J. *J. Phys. Org. Chem.* **1993**, *6*, 523. (c) Bourne, S.; Modro, A. M.; Modro, T. A. *Phosphorus, Sulfur Silicon* **1995**, *102*, 83.

(23) Ta-Shma, R.; Schneider, H.; Mahajana, M.; Katzhendler, J.; Breuer, E. *J. Chem. Soc., Perkin Trans. 2* **2001**, 1404.

(24) (a) Abraham , M. H.; Duce, P. P.; Pirov, D. V.; Barratt, D. G.; Morris, J. J.; Taylor, P. J. *J. Chem. Soc., Perkin Trans. 2* **1989**, 1355. (b) Hickey, J. P.; Passino-Reader, D. *R. Environ. Sci. Technol.* **1991**, *25*, 1753. (c) Raevsky, O. A.; Grigor'ev, V. Y.; Kireev, D. B.; Zefirov, N. S. *Quant. Struct. Act. Relat.* **1992**, *11*, 49.

TABLE 7. Comparison of K_{enol} Values for Dialkoxyphosphinyl- and Ester-Activated Carboxamides in Different Solvents at 298 K

$(MeO)_2P(=O)CH(CO_2R)CONHX$ and $MeOCOCH(CO_2R)CONHX$

R	X	solvent	K_{enol}^P	K_{enol}^E	K_{enol}^P/K_{enol}^E
Me	Ph	$CDCl_3$	0.098	0.05[a]	1.96
	i-Pr	CCl_4	1.10	1.4[b]	0.79
		$CDCl_3$	0.16	0.1[b]	1.6
		CD_3CN	0.041	≤0.01[b]	≥4.1
CH_2CF_3	*p*-An	CCl_4	9.0	3.5[c]	2.57
		$CDCl_3$	1.26	0.52[c]	2.42
		CD_3CN	0.15	≤0.02[c]	≥7.5
	Ph	CCl_4	6.8	2.3[c]	2.96
		$CDCl_3$	1.07	0.35[c]	3.06
		CD_3CN	0.11	≤0.02[c]	≥5.5
	i-Pr	CCl_4	10.8	10.1[b]	1.07
		$CDCl_3$	1.74	1[b]	1.74
		CD_3CN	0.38	≤0.01[b]	≥38
$CH(CF_3)_2$	*p*-An	CCl_4	61.5	≥50[c]	≤1.23
		$CDCl_3$	14.9	4.9[c]	3.04
		CD_3CN	1.5	≤0.02[c]	≥75
	Ph	CCl_4	51.6	13.2[c]	3.91
		$CDCl_3$	12.9	3.8[c]	3.39
		CD_3CN	1.10	≤0.02[c]	≥55

$(CF_3CH_2O)_2P(=O)CH(CO_2R)CONHX$ and $(CF_3CH_2O)COCH(CO_2R)CONHX$

R	X	solvent	K_{enol}^P	K_{enol}^E	K_{enol}^P/K_{enol}^E
Me	*p*-An	CCl_4	6.58	3.5[c]	1.88
		$CDCl_3$	1.05	0.52[c]	2.02
		CD_3CN	0.09	≤0.02[c]	≥4.5
	Ph	CCl_4	5.25	2.3[c]	2.28
		$CDCl_3$	0.93	0.35[c]	2.66
		CD_3CN	0.07	≤0.02[c]	≥3.5
	i-Pr	CCl_4	10.7	10.1[b]	1.06
		$CDCl_3$	1.76	1.0[b]	1.76
		CD_3CN	0.21	≤0.01[b]	≥21
CH_2CF_3	*p*-An	CCl_4	44.5	≥50	≤0.89
		$CDCl_3$	15.7	7.3[c]	2.15
		CD_3CN	0.48	0.08[c]	6
	Ph	CCl_4	32.3	32[c]	1.01
		$CDCl_3$	11.5	6.7[c]	1.72
		CD_3CN	0.35	0.05[c]	7

[a] ref 4. [b] ref 7b. [c] ref 5.

competition.[18] It was concluded that the P=O group is a strong hydrogen bond acceptor and with respect to phenol it is ca. 100-fold more effective than a C=O group. As shown above, this preference is an important factor in determining the configuration of our enols.

Dialkoxyphosphinyl vs Ester Comparison. There are many systematic K_{enol} values, *E*/*Z* ratios and structural information from our previous work on diester-activated enols **3**,[4,5,7c] which are analogs of systems **6**/**7**, **9**/**10**, and **17**/**18**. This enables comparisons with systems such as **3**, $R^1 = CO_2Me$, and evaluation of the effect of, e.g., replacing a CO_2Me group by a $(MeO)_2P(=O)$ group. Comparative data are given in Table 7 where K_{enol}^P and K_{enol}^E are the equilibrium constants for the compared phosphonate and ester groups, respectively.

For a system with a constant CO_2Me group, the $K_{enol}(O=P(OMe)_2)/K_{enol}(CO_2Me)$ ratios are ca. 1.96 for X = Ph in $CDCl_3$, and 0.79, 1.6 and ≥4.1 for X = *i*-Pr in CCl_4, $CDCl_3$, and CD_3CN, respectively. For a constant $CO_2CH_2CF_3$ group, the $K_{enol}(O=P(OMe)_2)/K_{enol}(CO_2Me)$ ratios in the same solvents are 2.96, 3.06, ≥5.5 when X = Ph, 2.57, 2.42, and ≥7.5 when X = *p*-An, and 1.07, 1.74, and ≥38 when X = *i*-Pr, respectively. For a constant $CO_2CH(CF_3)_2$ group, the ratios in CCl_4, $CDCl_3$, and CD_3CN are 3.91, 3.39, and ≥55 for X = Ph, and ≤1.23, 3.04, and ≥75 for X = *p*-An, respectively.

In most cases, $K_{enol}[(MeO)_2P=O] > K_{enol}[MeOC=O]$ when the other group is constant. From the data quoted above the $O=P(OMe)_2$ group is a better H-bond acceptor and EWG and hence a better enol stablizing group than CO_2Me, and more so when the number of fluorines in the other ester group increases.

Such comparison may be misleading since the K_{enol} values are composite. A dissection to the values for the *E*- and *Z*-configurations is required and similar configurations of the $(MeO)_2P=O$ and CO_2Me derivatives should be compared. The major *Z*-enol of the phosphonate has a similar configuration to the major *E*-enol of the ester because both $(MeO)_2P=O$ and CO_2Me are cis to the OH. The $K_{enol}^P(Z)/K_{enol}^E(E)$ values (data not shown) also support the conclusion that a $O=P(OMe)_2$ is a better enol stabilizing group than CO_2Me.

We did not find σ values for the $CO_2CH_2CF_3$ and $CO_2CH(CF_3)_2$ groups, but the gas-phase data show that $\Delta G°$ acidity values for $CH_2(CO_2Me)_2$ and $CH_2(CO_2Me)CO_2CH_2CF_3$ are 341.3 and 333.5, respectively. We have no data for the hexafluoro-substituted ester, but for $CH_2(CN)CO_2R$ the $\Delta G°$ values are 334.5, 324.7 and 317.5 for R = Me, CF_3CH_2 and $CH(CF_3)_2$, respectively.[25] Hence, the fluorinated esters are expected to be equal or better than $O=P(OMe)_2$ as enol promoting groups.

In CCl_4 and $CDCl_3$, $K_{enol}^P < K_{enol}^{3-F}$, K_{enol}^{6-F} (these designations relate to the enols of fluorinated esters). In most cases, the $K_{enol}^P/K_{enol}^{3-F}$ and $K_{enol}^P/K_{enol}^{6-F}$ ratios are 0.12−0.28 and 0.022−0.045, respectively, and even close to zero due to complete enolization of some fluorinated ester derivatives. Consequently, the fluorinated esters are equal or better than $O=P(OMe)_2$ as enol stabilizing groups. However, in CD_3CN the $K_{enol}^P/K_{enol}^{3-F}$ values are 1.48−4.8 (for constant CO_2Me group they are >0.6 and 0.75 for X = Ph and *p*-An, respectively). $K_{enol}^P/K_{enol}^{6-F}$ values are ≥0.48. The values in CD_3CN (including K_{enol}^P/K_{enol}^E) are much larger than the corresponding values in CCl_4 and $CDCl_3$. It is not simple to explain the difference in term of solvation since four species (enol and amide in two solvents) are involved in the comparison. In the more polar DMSO-d_6, enols of the *N*-*i*-Pr and *N*-*t*-Bu derivatives of $(MeO)_2P(=O)CH(CO_2CH(CF_3)_2)CONHX$ are observed at 298 K with K_{enol} = 0.33 and 0.19, respectively. In DMSO-d_6/CCl_4 (v/v) mixtures the % of *E*- and *Z*-enol of **6o** decreases on addition of DMSO-d_6. At 0.08:1, 0.5:1, and 1:1 ratios, the % *E*-enol and % *Z*-enol are *ca.* 7.8 and 84.5, 0 and 61.2, 0 and 43.1, respectively. The data also indicate that the *Z*-isomer is more stable than the *E*-isomer and is even present in DMSO-d_6.

DFT Calculations. The relative free energies and geometries of the amide and the two enols (cf. Table S5 in the Supporting Information) and the K_{enol} values were calculated at B3LYP/6-31G** for the *N*-Ph derivatives **6b/7b**, **6g/7g** and **6l/7l**, for the cyano(phosphonate) derivative **9b/10b** and for the bis-(phosphonate)acetanilide **12b/13b**. The enol with a hydrogen-bonded OH to the C=O of ester group is the most stable species ***E*-7b,** being 1.4 kcal/mol more stable than the enol ***Z*-7b** and 4.1 kcal/mol more stable than the most stable amide conformer **6b**. The pK_{enol} values at 298 K are −3.0 and −2.0 for the *E*- and *Z*- enols, respectively. Substitution by three or six fluorine atoms inverts the stability and the ***Z*-7g** is 1.7 kcal/mol more stable than ***E*-7g** and 7.4 kcal/mol more stable than the amide. The pK_{enol}s are −5.4 and −4.2, respectively. Likewise, ***Z*-7l** is 0.5 and 6.9 kcal/mol more stable than ***E*-7l** and amide **6l**, respectively and the derived pK_{enol}s are −5.1 and −4.7. In

(25) Mishima, M.; Matsuoka, M.; Lei, Y. X.; Rappoport, Z. *J. Org. Chem.* **2004**, *69*, 5947.

(26) Frey, J.; Rappoport, Z. Z. *J. Org. Chem.* **1997**, *62*, 8327.

contrast, the amides **9b** and **12b** are calculated to be the more stable species, by 1.6 and 5.7 kcal/mol than **10b** and **13b**, respectively.

In order to evaluate the effect of the $(MeO)_2P{=}O$ and CO_2Me reactions on both components of the enolization equilibria the energies of the isodesmic reactions 6−9 were calculated when R = $(MeO)_2P{=}O$ and CO_2Me. In eqs 6 and 8, the CONHPh group is transferred from the amide **6** to CH_4

$$(MeO)_2POCHRCONHPh + CH_4 \rightleftharpoons CH_3CONHPh + (MeO)_2POCH_2R \quad (6)$$

$$(MeO)_2POCR{=}C(OH)NHPh + CH_4 \rightleftharpoons CH_2{=}C(OH)NHPh + (MeO)_2POCH_2R \quad (7)$$

$$(MeO)_2POCHRCONHPh + CH_2{=}CH_2 \rightleftharpoons CH_3CONHPh + (MeO)_2POCR{=}CH_2 \quad (8)$$

$$(MeO)_2POCR{=}C(OH)NHPh + CH_2{=}CH_2 \rightleftharpoons CH_2{=}C(OH)NHPh + (MeO)_2POCR{=}CH_2 \quad (9)$$

or to $CH_2{=}CH_2$, formally eliminating the interaction between the enolizing amide and the activating groups. In eqs 7 and 9 the transfer is similar from the precursor enol.

The ΔG values for R = $(MeO)_2P{=}O$ are 0.0, 24.5, 0.8 and 25.3 kcal/mol for eqs 6−9, respectively, and the corresponding values for R = CO_2Me are −2.2, 32.1, −7.6 and 26.7 kcal/mol, respectively. Hence, the main stabilizing interaction in the **6b**/**7b** system is of the enol species, which is larger for R = CO_2Me than for R = $(MeO)_2P{=}O$. Equation 10, which is the difference between eqs 6 and 7, or 8 and 9 gives the calculated energetics of the equilibria between **6b** and **7b** relative to the enolization of acetanilide.

$$(MeO)_2POCHRCONHPh + CH_2{=}C(OH)NHPh \rightleftharpoons CH_3CONHPh + (MeO)_2POCR{=}C(OH)NHPh \quad (10)$$

The ΔG values of reaction 10 are −24.5 and −34.3 kcal/mol for R = $(MeO)_2P{=}O$ and CO_2Me, respectively, i.e., enolization of the bis phosphonate derivative is much less favored than that of the phosphonate ester derivative, in line with the experimental observations.

From the isodesmic data the difference arises from the interaction between the C=C bond and the MeOCO (vs $(MeO)_2P{=}O$) rather than from the interaction between the C=C−OH and the MeOCO (vs $(MeO)_2P{=}O$) (see eq 8), i.e., the $[(MeO)_2P{=}O]_2C{=}C$ moiety is less stable than the $[(MeO)_2P{=}O](CO_2Me)C{=}C$ moiety.

Note that the increase in K_{enol} on substituting with fluorine atoms follows the experimental trend, although the close similarity between the CF_3 and the $(CF_3)_2$ derivatives is not observed in the experiment. Few attempted correlations between the observed and the calculated pK_{enol} values for enols **7b**, **7g**, **7l**, and **10b** were attempted. The correlation between pK_{enol}(calcd) and the observed pK_{enol} is close to half a parabola for the four available points when either the overall experimental pK_{enol}(total) (= $-\log[K(_{E-enol}) + K(_{Z-enol})]$) or the observed vs calculated p$K(_{E-enol})$ or p$K(_{Z-enol})$ are used. Attempted correlations of observed pK_{enol} (total) vs calculated pK_{enol}(total) and observed p$K(_{Z-enol})$ vs calculated pK$(_{Z-enol})$ and observed pK_{enol} (total) vs calculated pK$(_{Z-enol})$ gave R^2 values of 0.639, 0.696, and 0.754, respectively. In contrast, a linear correlation of the observed K_{enol}(total) or the observed $K(_{E-enol})$ vs the calculated $K(_{E-enol})$ value for the three available points are linear with slopes of 0.80 (R^2 = 0.9414) and 1.02 (R^2 = 0.9451), respectively (Figure 6).

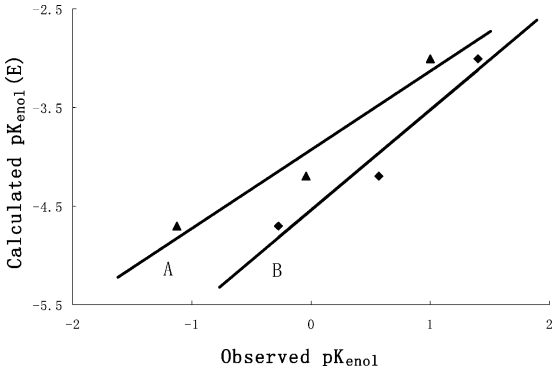

FIGURE 6. Correlations of the observed pK_{enol}(total) or the observed p$K(_{E-enol})$ vs the calculated p$K(_{E-enol})$: (A) calcd p$K(_{E-enol})$ vs obsd pK_{enol}(total), $y = 0.798x - 3.923$ ($R^2 = 0.9414$); (B) calcd p$K(_{E-enol})$ vs obsd p$K(_{E-enol})$, $y = 1.019x - 4.54$ ($R^2 = 0.9451$).

Conclusions. Carboxamides $(R'O)_2P(=O)CH(CO_2R)CONHX$ (R = Me, CF_3CH_2, $(CF_3)_2CH$, R′ = Me, CF_3CH_2) appear in CCl_4, $CDCl_3$, THF-d_8, and CD_3CN solutions as mixtures of amide and the *E*- and *Z*-enols, and in DMSO-d_6 mostly as the amides. $\delta(^1HO)$ values of the *E*-enols when R = Me are at the lowest field and $\Delta\delta$(OH) (*E*-enol − *Z*-enol) are at ca. 1.6 ppm to a higher field. When R = CF_3CH_2 and $(CF_3)_2CH$ $\Delta\delta$(OH) decrease by ca. 1 and 2 ppm, respectively, and for R = $(CF_3)_2$-CH δ(OH, *Z*-enol) > δ(OH, *E*-enol). The *Z*-enols are more abundant (stable) than the *E*-enol by 0.17−1.8 kcal/mol for **6**/**7** and **17e**−**h**/**18e**−**h** and less abundant than the *E*-enol by −0.3 to −0.13 kcal/mol for **17a**−**d**/**18a**−**d**. Except when R′ is CF_3CH_2, the % of the *E*-enol in the *E*/*Z* mixtures is linear with $\Delta\delta$(OH) value. Analysis of the δ(OH), δ(NH), $\delta(^{13}C)$, $\delta(^{19}F)$, and $\delta(^{31}P)$ values indicate that for each enol there are two simultaneously hydrogen bonds O−H···O=M and N−H···O=M with M = C and M = P. The hydrogen bond strengths follow the order for P=O > C=O, they decrease when the number of F atoms in R increase, and they are responsible for the configurations of the enols. The solid-state structure when R = R′ = Me is that of the amide, but when R = $(CF_3)_2CH$, R′ = Me it is the *Z*-enol. $[(MeO)_2PO]_2CHCONHX$ form only the amides in solution, and $(MeO)_2POCH(CN)CONHX$ form only the Z-enol in ≤7.3%. DFT calculations confirm the experimental trends, but the K_{enol} values differ somewhat from the experimental values.

The general message is that the effect of $O{=}P(OR')_2$ groups on the extent of enolization of a CONHX group is mostly, but not always, consistent with conclusions obtained earlier with other activating groups, especially CO_2R. The changes in K_{enol} values by fluorine substitution, or by the change in the solvent are determined by the EW ability and especially by the hydrogen bond accepting ability of the activating group. The latter effect when applies to the simultaneous hydrogen bonding to the OH and NH groups of the enol predominates in determining the *E*/*Z* enol ratios. On the other hand, caution should be exercised in extrapolation from well understood systems to slightly less understood ones, e.g., from the close analogy between $O{=}P(OR')_2$, CO_2R'-substituted systems and two ester systems where a single $O{=}P(OMe)_2$ group is a better activator to enol formation than a single CO_2Me, to a doubly activated system where two CO_2Me groups are better activators than two $O{=}P(OMe)_2$ groups. Likewise, a CN, $O{=}P(OMe)_2$ activated system is less enolic than a CN, CO_2Me activated system. Hence, effects such as steric crowding should be also taken into account. The overall

TABLE 8. Analytical Data and Melting Points for All Amide/Enol Systems

			calcd, %			found, %		
compd	formula	mp, °C	C	H	N	C	H	N
6a/7a	$C_{13}H_{18}NO_7P$	108−110	47.13	5.44	4.23	47.40	5.44	4.16
6b/7b	$C_{12}H_{16}NO_6P$	85−8	47.84	5.32	4.65	47.97	5.37	4.44
6c/7c	$C_{12}H_{11}F_5NO_6P$	98−101	36.83	2.81	3.58	36.76	2.88	3.43
6d/7d	$C_9H_{18}NO_6P$	53−5	40.45	6.74	5.24	40.44	6.69	5.04
6e/7e	$C_{10}H_{20}NO_6P$	73−5	42.70	7.12	4.98	42.83	7.12	4.92
6f/7f	$C_{14}H_{17}F_3NO_7P$	138−140	42.11	4.26	3.51	42.45	4.35	3.31
6g/7g	$C_{13}H_{15}F_3NO_6P$	61−3	42.28	4.07	3.79	42.52	4.34	3.46
6h/7h	$C_{13}H_{10}F_8NO_6P$	104−7	33.99	2.18	3.05	34.20	2.26	2.88
6i/7i	$C_{10}H_{17}F_3NO_6P$	46−7	35.82	5.07	4.18	35.65	5.18	4.23
6j/7j	$C_{11}H_{19}F_3NO_6P$	60−3	37.82	5.44	4.01	38.13	5.58	3.78
6k/7k	$C_{15}H_{16}F_6NO_7P$	92−4	38.54	3.43	3.00	38.83	3.41	2.94
6l/7l	$C_{14}H_{14}F_6NO_6P$	74−7	38.44	3.20	3.20	38.76	3.13	3.12
6m/7m	$C_{14}H_9F_{11}NO_6P$	104−7	31.88	1.71	2.66	32.14	1.92	2.56
6n/7n	$C_{11}H_{16}F_6NO_6P$	90−2	32.75	3.97	3.47	33.03	3.95	3.44
6o/7o	$C_{12}H_{18}F_6NO_6P$	113−6	34.53	4.32	3.36	34.73	4.03	3.36
9a/10a	$C_{12}H_{15}N_2O_5P$	155−7	48.32	5.03	9.40	48.72	5.13	9.10
9b/10b	$C_{11}H_{13}N_2O_4P$	120−2	49.25	4.85	10.45	49.28	4.91	10.20
9c/10c	$C_{11}H_8F_5N_2O_4P$	152−4	36.87	2.23	7.82	37.03	2.29	7.69
9d/10d	$C_9H_{17}N_2O_4P$	164−6	43.55	6.85	11.29	43.68	6.81	11.14
12a/13a	$C_{13}H_{21}NO_8P_2$	152−4	40.95	5.58	3.67	41.04	5.57	3.65
12b/13b	$C_{12}H_{19}NO_7P_2$	109−111	41.03	5.45	3.90	41.17	5.43	3.69
12c/13c	$C_{12}H_{14}F_5NO_7P_2$	112−4	32.67	3.20	3.18	32.74	3.01	2.89
12d/13d	$C_9H_{21}NO_7P_2$	86−8	34.08	6.67	4.42	34.22	6.77	4.40
12e/13e	$C_{10}H_{23}NO_7P_2$	62−4	36.26	7.00	4.23	35.98	7.07	4.18
17a/18a	$C_{15}H_{16}F_6NO_7P$	96−8	38.55	3.45	3.00	38.72	3.33	2.90
17b/18b	$C_{14}H_{14}F_6NO_6P$	98−100	38.46	3.23	3.20	38.63	3.03	2.94
17c/18c	$C_{11}H_{16}F_6NO_6P$	101−2	32.77	4.00	3.47	32.89	3.73	3.21
17d/18d	$C_{12}H_{18}F_6NO_6P$	96−8	34.54	4.35	3.36	34.43	4.12	3.23
17e/18e	$C_{16}H_{15}F_9NO_7P$	82−4	35.90	2.82	2.62	35.74	2.71	2.56
17f/18f	$C_{15}H_{13}F_9NO_6P$	94−95	35.66	2.59	2.77	35.81	2.66	2.61
17g/18g	$C_{12}H_{15}F_9NO_6P$	69−70	30.59	3.21	2.97	30.30	3.03	2.88
17h/18h	$C_{13}H_{17}F_9NO_6P$	67−9	32.18	3.53	2.89	31.24	3.17	2.27

effects affect the relative $K_{enol}(O{=}P(OR')_2)/K_{enol}(CO_2R)$ ratios for enol formation.

An important conclusion is that the previously used rule that the lowest δ(OH) value is always associated with the most abundant isomer does not always apply. Analysis of the appropriate hydrogen bonds should replace the formal "rule".

The present work also demonstrates the ability of inverting the order of stability of *E*- and *Z*-isomers by proper substitution. They also show that the $O{=}P(OR')_2$ substituent is a suitable activator for enolization since no competing enolization on the P═O group was found.

Experimental Section

General Methods. Melting points were uncorrected, ^1H and ^{13}C NMR spectra were recorded as described previously.[8]

Solvents and Materials. CCl_4, $CDCl_3$, THF-d_8, CD_3CN, DMSO-d_6, and the precursors for the synthetic work were purchased from a commercial supplier and were used without further purification.

Analytical and Spectral Data. Melting points and microanalysis data are given in Table 8.

Selected ^1H, ^{13}C, ^{19}F, and ^{31}P NMR spectra in the various solvents studied are given in Tables 2−4, and the full data are given in Tables S1−S3 in the Supporting Information.

Reaction of Dimethyl Phosphonoacetate with Organic Isocyanates XNCO To Form 6a−e/7a−e. Na pieces (48 mg, 2.1 mmol) were added to the solution of dimethyl phosphonoacetate (364 mg, 2 mmol) in dry THF (5 mL) for **6d,e** or in Et_2O (20 mL) for **6a** at 0 °C, and the mixture was stirred for *ca.* 6 h at 0 °C and for additional 18 h at rt. To this solution the isocyanate (2 mmol) in THF (1 mL) was added dropwise at 0 °C, and the mixture was stirred for about 12 h and for additional 12 h at rt. (a) For **6a** and **6d**−**e**, the precipitate formed in the reaction solution was filtered, and washed with little Et_2O to give the Na salts of **6a** (0.72 g), of **6d** (0.45 g) or of **6e** (0.32 g). A solution of the salt in DMF (2−4 mL) was added dropwise to ice-cooled 2 N HCl solution (20−40 mL) and kept overnight at 4 °C. The solution was extracted with EtOAc, washed with brine, and dried over Na_2SO_4. After evaporation of the solvent the residue was crystallized from EtOAc-petroleum ether (40−60 °C) to afford 0.25 g (38%) of **6a**, 0.30 g (56%) of **6d**, or 0.21 g (37%) of **6e** as light yellow or white powders.

(b) No precipitate was formed for **6b**,**c** in the solution, and the solution was directly added to ice-cooled 2 N HCl (40 mL), and then followed procedure (a) above in order to obtain 0.26 g (43%) of **6b** or 0.28 g (36%) of **6c** as a white or pale yellow powder.

Analyses and NMR data are given in Table 8 and Tables S1−S3 in Supporting Information.

2,2,2-Trifluoroethyl Chloroacetate. The compound was prepared by two methods.

(a) Chloroacetic acid (9.45 g,100 mmol) was refluxed for 12 h in benzene (30 mL) containing excess 2,2,2-trifluoroethanol (11 g, 110 mmol) and 98% H_2SO_4 (6 g) in a 100 mL round flask attached to a Dean−Stark trap. The solution was washed with saturated Na_2CO_3 (3 × 20 mL) and brine (3 × 10 mL) and dried (Na_2SO_4). Distillation of the crude product afforded 2.4 g (13.6%) of the colorless ester, bp 124−126 °C.

(b) To a solution of 2,2,2-trifluoroethanol (26.4 g, 264 mmol) in CH_2Cl_2 (70 mL) was added dropwise triethylamine (24.32 g, 240 mmol) during 15 min, and then chloroacetyl chloride (27.15 g, 240 mmol) in CH_2Cl_2 (70 mL) was added dropwise during 30 min. The solution was refluxed for 2 h and stirred overnight at rt. The formed triethylammonium salt was removed by filtration, and the filtrate was washed successively with 2 N HCl (2 × 50 mL) and saturated Na_2CO_3 (2 × 20 mL) and dried (Na_2SO_4). The solvent was evaporated, the crude product was distilled and the fraction with boiling range of 120−126 °C (23 g, 54%) was collected.

^1H NMR ($CDCl_3$, 298K) δ: 4.56 (q, $^3J_{HF}$ = 8.28 Hz, 2H, CH_2-CF_3), 4.19 (s, 2H, CH_2Cl). The compound is relatively unstable, and satisfactory elemental analysis could not be obtained.

2,2,2-Trifluoroethyl Phosphonoacetate. A mixture of 2,2,2-trifluoroethyl chloroacetate (23 g, 130 mmol) and trimethyl

phosphite (17.8 g, 144 mmol) was heated at ca. 80 °C for 48 h. The volatile components were evaporated under reduced pressure and the residue was purified by column chromatography (silica, EtOAc) giving 15.6 g (48%) of a liquid colorless 2,2,2-trifluoroethyl phosphonoacetate. ^{1}H NMR ($CDCl_3$, 298 K), δ: 4.51 (q, $^3J_{HF}$ = 8.33 Hz, 2H, CH_2CF_3), 3.80 (d, $^3J_{PH}$ = 12.26 Hz, 6H, CH_3O), 3.59 (d, $^2J_{PH}$ = 21.62 Hz, 2H, CH_2P). ^{19}F NMR ($CDCl_3$, 298 K) δ: −74.60 (t, $^3J_{HF}$ = 7.9 Hz, CF_3). ^{31}P NMR ($CDCl_3$, 298 K) δ: 20.59 (t of hept, $^2J_{PH}$ = 21.61 Hz, $^3J_{PH}$ = 11.10 Hz). ^{13}C NMR ($CDCl_3$, 298 K) δ: 164.2 (d of m, $^2J_{CP}$ = 6.1 Hz, CO), 122.6 (q of t, J_{CF} = 277.1 Hz, $^2J_{CH}$ = 4.8 Hz, CF_3), 61.0 (t of q, J_{CH} = 151.3 Hz, $^2J_{CF}$ = 37.0 Hz, *C*H_2CF_3), 53.3 (q of d, J_{CH} = 148.6 Hz, $^2J_{CP}$ = 6.4 Hz, CH_3O), 32.8 (d of t, J_{CP} = 135.1 Hz, J_{CH} = 130. 9 Hz, CH_2PO).

Anal. Calcd for $C_6H_{10}F_3O_5P$: C, 28.80; H, 4.00. Found: C, 28.75; H, 4.08.

Reaction of 2,2,2-Trifluoroethyl Phosphonoacetate with Organic Isocyanates To Give 6f−j. Na pieces (48 mg, 2.1 mmol) were added to a solution of 2,2,2-trifluoroethyl phosphonoacetate (500 mg, 2 mmol) in dry THF (4 mL) at 0 °C, and the solution was stirred for ca. 6 h and for an additional 8 h at rt. To this solution was added the isocyanate solution (2 mmol) in THF (1 mL) dropwise at 0 °C, and the mixture was stirred for ca. 18 h and an additional 6 h at rt. (a) For **6f** and **6h**, the solution was then poured into ice-cooled 2 N HCl solution (50 mL) and kept overnight at 4 °C. The precipitate formed was filtered, washed with cold water, and dried in air giving 0.36 g (45%) of a white powder of **6f** or 0.54 g (59%) of a light yellow powder of **6h**. A white analytical sample was crystallized from EtOAc−petroleum ether (40−60 °C).

(b) For **6g** and **6i**, the solution was poured into ice-cooled 2 N HCl solution (50 mL) and then extracted with CH_2Cl_2, washed with brine, and dried (Na_2SO_4). Evaporation of the solvent afforded 0.65 g (88%) of a light yellow powder of **6g**, or 0.35 g (52%) of a light yellow oil of **6i**, which solidified at −20 °C after standing for a long time. A colorless analytical sample was crystallized from EtOAc−petroleum ether (40−60 °C).

(c) For **6j**, the precipitate formed in the solution was filtered, washed with little Et_2O to give the Na salt of **6j** (0.25 g, 34%). The salt was dissolved in DMF (1 mL) and added dropwise to an ice-cooled 2 N HCl solution (10 mL) and kept overnight at 4 °C. The solution was extracted with EtOAc, washed with brine and dried (Na_2SO_4). The solvent was evaporated and the residue was crystallized from EtOAc-petroleum ether (40−60 °C), giving 0.19 g (27%) of a white powder of **6j**.

Analyses and NMR data are given in Table 8 and Tables S1−S3 in the Supporting Information.

1,1,1,3,3,3-Hexafluoro-2-propyl Chloroacetate. To the solution of 1,1,1,3,3,3-hexafluoro-2-propanol (24.5 g, 146 mmol) in CH_2Cl_2 (65 mL) at 0 °C was added dropwise triethylamine (14.7 g, 146 mmol) during 15 min. Chloroacetyl chloride (18.3 g, 162 mmol) in CH_2Cl_2 (65 mL) was then added dropwise during 1 h, and the solution was stirred at 0 °C for ca. 6 h and then overnight at rt. The formed triethylammonium salt was removed by filtration, and the filtrate was washed successively with 2 N HCl solution (2 × 30 mL) and saturated Na_2CO_3 solution (2 × 20 mL) and dried (Na_2SO_4). The solvent was evaporated, the crude product was distilled and the fraction with boiling range of 104−108 °C (21.6 g, 61%) was collected.

^{1}H NMR ($CDCl_3$, 298 K) δ: 5.78 (hept, $^3J_{HF}$ = 5.93 Hz, 1H, $CHCF_3$), 4.24 (s, 2H, CH_2Cl). ^{13}C NMR ($CDCl_3$, 298 K) δ: 164.8 (m, CO), 120.1 (q of m, $^1J_{CF}$ = 282.3 Hz, CF_3), 67.6 (d of hept, $^1J_{CH}$ = 151.2 Hz, $^2J_{CF}$ = 35.1 Hz, CH), 39.5 (t, $^1J_{CH}$ = 152.8 Hz, CH_2). The compound is relatively unstable, and satisfactory elemental analysis could not be obtained.

1,1,1,3,3,3-Hexafluoro-2-propyl Phosphonoacetate. A mixture of 1,1,1,3,3,3-hexafluoro-2-propyl chloroacetate (21.6 g, 88 mmol) and trimethyl phosphite (12.0 g, 97 mmol) was heated at ca. 80 °C for ca. 48 h. The volatile components were evaporated under reduced pressure, and the residue was purified by column chromatography (silica, EtOAc) giving 9.64 g (34%) of the colorless liquid 1,1,1,3,3,3-hexafluoro-2-propyl chloroacetate. ^{1}H NMR ($CDCl_3$, 298 K) δ: 5.70 (hept, $^3J_{HF}$ = 6.01 Hz, 1H, CH), 3.71 (d, $^3J_{PH}$ = 11.41 Hz, 6H, CH_3O), 3.08 (d, $^2J_{PH}$ = 22.00 Hz, 2H, CH_2). ^{19}F NMR ($CDCl_3$, 298 K) δ: −74.45 (d, $^3J_{HF}$ = 6.1 Hz, CF_3). ^{31}P NMR ($CDCl_3$, 298 K) δ: 19.00 (t of hept, $^2J_{PH}$ = 21.54 Hz, $^3J_{PH}$ = 11.58 Hz). ^{13}C NMR ($CDCl_3$, 298 K) δ: 162.8 (d of m, $^2J_{CP}$ = 6.8 Hz, CO), 120.1 (q of m, J_{CF} = 283.0 Hz, CF_3), 66.9 (d of hept, J_{CH} = 151.0 Hz, $^2J_{CF}$ = 35.1 Hz, CH), 53.1 (q of d, J_{CH} = 148.8 Hz, $^2J_{CP}$ = 6.3 Hz, CH_3O), 33.3 (t of d, J_{CH} = 131.8 Hz, J_{CP} = 133.7 Hz, C*H*-PO).

Anal. Calcd for $C_7H_9F_6O_5P$: C, 26.42; H, 2.83. Found: C, 26.26; H, 2.88.

Reaction of 1,1,1,3,3,3-Hexafluoro-2-propyl Phosphonoacetate with Organic Isocyanates To Form 6k-o. The procedure with phenyl isocyanate is also representative of the reactions of the *p*-An, C_6F_5, *t*-Bu, and *i*-Pr isocyanates.

Sodium (48 mg, 2.1 mmol) was added to the solution of 1,1,1,3,3,3-hexafluoro-2-propyl phosphonoacetate (636 mg, 2 mmol) in dry THF (4 mL) at 0 °C, and the mixture was stirred for 12 h. A solution of phenyl isocyanate (238 mg, 2 mmol) in THF (1 mL) was added dropwise at 0 °C, and the mixture was stirred for ca. 12 h and additional 12 h at rt. The precipitate was removed by filtration, and the filtrate was poured into ice-cooled 2 N HCl solution (50 mL) and kept overnight at 4 °C. The precipitate formed was filtered, washed with cold water and dried in air, giving 0.48 g (55%) of a white powder of **6l** which was crystallized from EtOAc-petroleum ether (40−60 °C). **6k** and **6m−o** were obtained similarly and their yields, analyses and NMR data are given in Table 8 and Tables S1−S3 in the Supporting Information.

Dimethoxyphosphinylacetonitrile. A mixture of chloroacetonitrile (6.04 g, 80 mmol) and trimethyl phosphite (10.92 g, 88 mmol) was heated at ca. 80 °C for 48 h. The volatile component was evaporated under reduced pressure and the residue was purified by column chromatography (silica, EtOAc), giving 3.6 g (30%) of colorless dimethoxyphosphinylacetonitrile which was solidified after storing at −20 °C.

Anal. Calcd for $C_4H_8NO_3P$: C, 32.21; H, 5.37; N, 9.40. Found: C, 32.82; H, 5.54; N, 8.66.

^{1}H NMR ($CDCl_3$, 298 K) δ: 3.69(d, $^3J_{PH}$ = 11.50 Hz, 6H, CH_3O), 2.85(d, $^2J_{PH}$ = 21.10 Hz, 2H, CH_2); ^{13}C NMR ($CDCl_3$, 298 K) δ: 112.3 (d of t, $^2J_{CP}$ = 11.4 Hz, $^2J_{CH}$ = 10.9 Hz, CN), 53.5 (q of d, J_{CH}= 149.2 Hz, $^2J_{CP}$ = 6.7 Hz, CH_3O), 14.7 (d of t, J_{CP} = 143.7 Hz, J_{CH} = 135.6 Hz, CH_2); ^{13}P NMR ($CDCl_3$, 298 K) δ: 17.03 (d of hept, $^2J_{PH}$ = 21.62 Hz, $^3J_{PH}$ = 11.29 Hz, PO).

Reaction of Dimethoxyphosphinylacetonitrile with Organic Isocyanates To Form 9a−d. Na (72 mg, 3.1 mmol) was added to a solution of dimethoxyphosphinylacetonitrile (447 mg, 3 mmol) in dry THF (5 mL) at 0 °C and the solution was stirred for ca. 6 h and then for additional 8 h at rt. To this solution the isocyanate (447 mg, 3 mmol) in THF (1 mL) was added dropwise at 0 °C, and the mixture was stirred for ca. 12 h and for additional 12 h at rt. It was then poured into ice-cooled 2 N HCl solution (60 mL) and kept for a few hours at 4 °C. (a) For **9a** and **9c**, a precipitate was formed in the aqueous solution, filtered, washed with cold water, and dried in air. Crystallization from EtOAc−petroleum ether (40−60 °C) afforded 0.19 g (21%) of white cotton-like solid **9a** or 0.56 g (51.7%) of the yellow solid **9c**.

(b) For **9b** and **9d**, no precipitate was formed in the aqueous solution, and the solution was extracted with EtOAc and dried (Na_2SO_4), and the solvent was evaporated. The remaining solid was crystallized from EtOAc−petroleum ether (40−60 °C), giving 0.51 g (63%) of a light yellow solid of **9b**, or 0.44 g (58.5%) of a light yellow powder of **9d**. Crystallization was from EtOAc.

Analyses and NMR data are given in Table 8 and Tables S1−S3 in the Supporting Information.

General Procedure for the Reaction of Tetramethyl Methylenebisphosphonate with Isocyanates to Form 12a−e. Na (72 mg, 3.1 mmol) was added to a solution of tetramethyl methylenebisphosphonate (696 mg, 3 mmol) in dry Et_2O (20 mL) at rt

and stirring continued until its complete disappearance. The organic isocyanate (3 mmol) in Et_2O (3 mL) was added dropwise at 0 °C, and the mixture was stirred for ca. 12 h at 0 °C and additional 12 h at rt. The solution was filtered and the Na salt was washed quickly with a small amount of Et_2O and suspended in Et_2O (10 mL). An ice-cooled 2 N HCl solution (50 mL) was poured into the suspension, which was then extracted with chloroform (3 × 20 mL), dried ($MgSO_4$) and the solvent was evaporated. The crude residue was crystallized from EtOAc-petroleum ether (40−60 °C), giving the desired compound (**12a-e**). Analyses and NMR data are given in Table 8 and Tables S1−S3 in the Supporting Information.

2,2,2-Trifluoroethyl Bis(2,2,2-trifluoroethyl)phosphonoacetate. To a solution of bis(2,2,2-trifluoroethyl) phosphonoacetate (5 g, 15.7 mmol) in 2,2,2-trifluoroethanol (32 g, 314 mmol) was added 98% sulfuric acid (0.8 g), and the solution was refluxed overnight. After cooling, the solution was added to saturated Na_2CO_3 solution (30 mL), and the organic layer at the bottom was separated. The aqueous layer was extracted twice with chloroform, and the combined organic layer was dried over anhydrous Na_2SO_4. Evaporation gave a 1:0.81 mol/mol mixture of the precursor and the desired esters (based on ^{1}H NMR). The mixture was separated by column chromatography (silica gel, 2:3 EtOAc/petroleum ether). The first fraction was collected and evaporation afforded 1.6 g (26%) of **16** as a colorless oil.

Anal. Calcd for $C_8H_8F_9O_5P$: C, 24.89; H, 2.09. Found: C, 25.69; H, 2.18.

^{1}H NMR ($CDCl_3$, 298 K) δ: 4.53 (q, $^3J_{HF}$ = 8.25 Hz, 2H, $CO_2CH_2CF_3$), 4.45 (m, 4H, CF_3CH_2OPO), 3.26 (d, $^2J_{PH}$ = 21.54 Hz, 2H, CH_2). ^{19}F−H coupled NMR ($CDCl_3$, 298 K) δ: −74.75 (t, $^3J_{HF}$ = 8.09 Hz, 3F, $CO_2CH_2CF_3$), −76.37 (t, $^3J_{HF}$ = 7.91 Hz, CF_3CH_2OPO). ^{13}C NMR ($CDCl_3$, 298 K) δ: 163.2 (dm, $^2J_{CP}$ = 4.8 Hz, CO), 122.4 + 122.3 + 122.2 (q of t, J_{CF} = 277.2 Hz, $^2J_{CH}$ = 4.6 Hz, CF_3), 62.7 (tqd, J_{CH} = 152.6 Hz, $^2J_{CF}$ = 38.4 Hz, $^2J_{CP}$ = 5.6 Hz, CF_3CH_2OPO), 61.3 (t of q, J_{CH} = 151.8 Hz, $^2J_{CF}$ = 37.3 Hz, $CO_2CH_2CF_3$), 33.4 (d of t, J_{CP} = 144.5 Hz, J_{CH} = 131.5 Hz, CH_2PO).

General Procedure for the Reaction of Bis(2,2,2-trifluoroethyl) Methoxycarbonylmethyl Phosphonate with Isocyanates to Give 17a−d. Na (48 mg, 2.1 mmol) was added to a solution of bis(2,2,2-trifluoroethyl) methoxycarbonylmethyl phosphonate (636 mg, 2 mmol) in dry Et_2O (20 mL) at rt with stirring which continued until complete disappearance of the Na. The organic isocyanate (2 mmol) in Et_2O (2 mL) was added dropwise at 0 °C, and the mixture was stirred for ca. 12 h at 0 °C and additional 12 h at rt. Ice-cooled 2 N HCl solution (40 mL) was poured into the solution, which was then extracted with chloroform (3 × 20 mL) and dried ($MgSO_4$), and the solvent was evaporated. The crude residue was crystallized with EtOAc−petroleum ether (40−60 °C) giving **17b−d**. The product **17a** of *p*-methoxyphenyl isocyanate was crystallized from CCl_4-petroleum ether. Analyses and NMR data are given in Table 8 and Tables S1−S3 in the Supporting Information.

General Procedure for the Reaction of 2,2,2-Trifluoroethyl Bis(2,2,2-trifluoroethyl) Phosphonoacetate with Isocyanates To Give 17e−h. Na (25 mg, 1.1 mmol) was added with stirring to a solution of 2,2,2-trifluoroethyl bis(2,2,2-trifluoroethyl)phosphonoacetate (386 mg, 1 mmol) in dry Et_2O (10 mL) at 0 °C and stirring continued until all of the Na disappeared. The organic isocyanate (1 mmol) in Et_2O (1 mL) was added dropwise at 0 °C, and the mixture was stirred for ca. 24 h at 0 °C. The solvent was evaporated and the remainder (except for **17g**) was washed with chloroform for **17e**,**f** or with benzene for **17h** and suspended in chloroform. Then 32% HCl (10−20 mL) containing ice (20 g) was poured into the suspension which was extracted with chloroform (3 × 20 mL) and dried ($MgSO_4$).The residue was crystallized from EtOAc−petroleum ether (40−60 °C) and gave the desired compound. Analyses and NMR data are given in Table 8 and Tables S1−S3 in the Supporting Information.

Computation Methods. The compounds investigated were optimized by using the Gaussian 98 program[27] at the hybrid density functional B3LYP/6-31G** method[28] which was extensively used in recent calculations of enols of carboxylic acid derivatives and shown to give pK_{enol} values reliable within 2 pK_{enol} units.[29] All optimized structures including higher energy conformers were confirmed by frequency analysis to be local minima on the potential energy surfaces. K_{enol} values were calculated from the free energy differences between the amide and enol forms at 298.15 K.

Acknowledgment. We are indebted to the Israel Science Foundation for support, to Dr. Shmuel Cohen from the Department of Inorganic and Analytical Chemistry, The Hebrew University, for the X-ray structure determination, and to Professors Tony Kirby, Marvin Charton, and Eli Breuer for discussions.

Supporting Information Available: Tables S1−S3 with complete ^{1}H, ^{13}C, ^{19}F, and ^{31}P NMR data, Table S4 with relative integration of signals for all compounds, and Table S5 for the calculated geometries of enols and amides. Full crystallographic data for the compounds in Table 1 and compounds **12d**, **17b**, **19**, and **20** (CIF). This material is available free of charge via the Internet at http://pubs.acs.org.

JO0710679

(27) Gaussian 98, Revision A.6: Frisch, M. J.; Trucks, G. W.; Schlegel, H. B.; Scuseria, G. E.; Robb, M. A.; Cheeseman, J. R.; Zakrzewski, V. G.; Montgomery, J. A., Jr.; Stratmann, R. E.; Burant, J. C.; Dapprich, S.; Millam, J. M.; Daniels, A. D.; Kudin, K. N.; Strain, M. C.; Farkas, O.; Tomasi, J.; Barone, V.; Cossi, M.; Cammi, R.; Mennucci, B.; Pomelli, C.; Adamo, C.; Clifford, S.; Ochterski, J.; Petersson, G. A.; Ayala, P. Y.; Cui, Q.; Morokuma, K.; Malick, D. K.; Rabuck, A. D.; Raghavachari, K.; Foresman, J. B.; Cioslowski, J.; Ortiz, J. V.; Stefanov, B. B.; Liu, G.; Liashenko, A.; Piskorz, P.; Komaromi, I.; Gomperts, R.; Martin, R. L.; Fox, D. J.; Keith, T.; Al-Laham, M. A.; Peng, C. Y.; Nanayakkara, A.; Challacombe, M.; Gill, P. M. W.; Johnson, B.; Chen, W.; Wong, M. W.; Andres, J. L.; Gonzalez, C.; Head-Gordon, M.; Replogle, E. S.; Pople, J. A. Gaussian, Inc., Pittsburgh, PA, 1998.

(28) (a) Becke, A. D. *Phys. Rev.* **1988**, *A38*, 3098. (b) Lee, C.; Yang, W.; Parr, R. G. *Phys. Rev.* **1988**, *B37*, 785.

(29) Apeloig, Y.; Arad, D.; Rappoport, Z. *J. Am. Chem. Soc*. **1990**, *112*, 9131. Sklenak, S.; Apeloig, Y.; Rappoport, Z. *J. Chem. Soc., Perkin Trans. 2* **2000**, 2269. Yamataka, H.; Rappoport, Z. *J. Am. Chem. Soc.* **2000**, *122*, 9818. Rappoport, Z.; Lei, Y. X.; Yamataka, H. *Helv. Chem. Acta* **2001**, *84*, 1401.